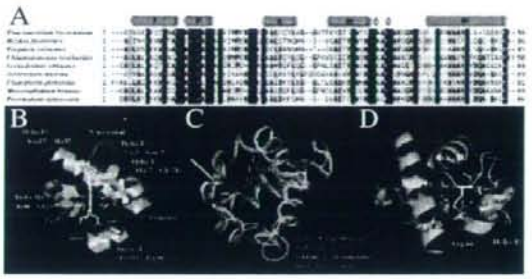

Fig. 2. Aligned Amino Acid Sequences of Cyts c_6 with Reported Crystal Structure and Crystal Structure of Diatom Ptc6.

A, The conserved and semi conserved amino-acid residues among the seven algal species and two cyanobacterial species are indicated by black and gray boxes respectively. The heme ligands, the residues forming the acidic patch, and the residues forming a salt-bridge are shown in yellow, red, and green respectively. The secondary structures of cyt c_6 of Ptc6 are indicated as follows: orange cylinders, α-helices; blue arrows, β-sheet. B, Overall structure of diatom Ptc6. The α-helix (marine) and β-sheet (green) are indicated using a cartoon model. The amino acid residues, heme group, and sulfate ions are represented by a stick model with atom-specific colors: white, carbon; blue, nitrogen; red, oxygen; yellow, sulfur; iron, orange. C, Superimposion of C^{α} traces of cyts c_6 of diatom *P. tricornutum* (purple; PDB code 3dmi), red alga *P. yezoensis* (red; PDB code 1gdv), green alga *C. reinhardtii* (green; PDB code 1cyj), and cyanobacteria *A. maxima* (marine; PDB code 1f1f). D, Salt-bridge of diatom Ptc6. Salt bridge is depicted by a broken line.

Monoraphidium braunii, *Cladophora glomerate*, *Scenedesmus obliquus*, *P. yezoensis*, *Hizikia fusiformis*, *Arthrospira maxima*, and *Phormidium laminosum* revealed identities of 56.7%, 47.19%, 41.76%, 50.6%, 55.7%, 56.7%, 55.6%, and 55.1% respectively (Fig. 2A). The C^{α} trace alignment of cyt c_6 from Ptc6, green alga *C. reinhardtii*,[14] red alga *P. yezoensis*,[12] and cyanobacteria *A. maxima*[15] is shown in Fig. 2C. The overall structure of Ptc6 was similar to the structures of algal and cyanobacterial cyt c_6 from red alga *P. yezoensis*,[12] green alga *C. reinhardtii*,[14] and cyanobacteria *A. maxima*,[15] with main-chain root mean square deviations of 0.8, 0.6, and 0.6 Å respectively using the DALI program.

A surface exposed salt bridge was formed among Arg44, Asp37, and Glu84 (Arg44NH1-Asp37$O^{\delta 1}$, 2.98 Å, Arg44NH2-Glu84$O^{\varepsilon 2}$, 2.89 Å) (Fig. 2D). Arg44 was conserved only in the diatom cyt c_6 (Fig. 2A), and this salt bridge has not been found in other cyts c_6 in the same region. Considering that a salt bridge of high binding energy contributes to the structural stability of a protein,[16] this salt-bridge of Ptc6 might contribute to the rigid packing of the interaction between helices II and IV and might increase the structural stability of the protein. Gdn-HCl cannot distinguish the contributions of electrostatic interaction such as a salt bridge, but the effects of a salt bridge are effectively monitored in urea, because the urea molecular is uncharged.[17] Urea denaturation experiments indicated that oxidized Ptc6 was more stable than red alga *P. yezoensis* cyt c_6. Hence, this salt bridge of Ptc6 may be one of the factors bringing it about that structural stability of Ptc6 is higher than that of red algal cyt c_6. This prediction is worthy of further study.

In this study, we determined the first crystal structure of diatom cyt c_6 at 1.5 Å resolution. The UV/vis spectra and redox potential of the protein were similar to those of other algal cyts c_6. The structural stability of Ptc6 was higher than that of red algal cyt c_6. Based on the results for crystal structure and for denaturation with urea of Ptc6, we estimated that this structural stability was to be attributed to a salt bridge, which was not found in other cyts c_6, among Arg44, Asp37, and Glu84 around helices II and IV.

Acknowledgment

This work was supported in part by the Nihon University College of Bioresource Sciences Research Fund for 2008.

References

1) Cavalier-Smith, T., Membrane heredity and early chloroplast evolution. *Trends Plant Sci.*, **5**, 174–182 (2000).
2) McFadden, G. I., Plastids and protein targeting. *J. Eukaryot. Microbiol.*, **46**, 339–346 (1999).
3) Peers, G., and Price, N. M., Copper-containing plastocyanin used for electron transport by an oceanic diatom. *Nature*, **441**, 341–344 (2006).
4) Shimazaki, K., Takamiya, K., and Nishimura, M., Studies on electron transfer systems in the marine diatom *Phaeodactylum tricornutum*. I. Isolation and characterization of cytochromes. *J. Biochem.*, **83**, 1631–1638 (1978).
5) Killian, O., and Kroth, P. G., Presequence acquisition during secondary endocytobiosis and the possible role of introns. *J. Mol. Evol.*, **58**, 712–721 (2004).
6) Akazaki, H., Kawai, F., Chida, H., Matsumoto, Y., Hirayama, M., Hoshikawa, K., Unzai, S., Hakamata, W., Nishio, T., Park, S.-Y., and Oku, T., Cloning, expression and purification of cytochrome c_6 from the brown alga *Hizikia fusiformis* and complete X-ray diffraction analysis of the structure. *Acta Crystallogr. F*, **64**, 674–680 (2008).
7) Satoh, T., Itoga, A., Isogai, Y., Kurihara, M., Yamada, S., Natori, M., Suzuki, N., Suruga, K., Kawachi, R., Arahira, M., Nishio, T., Fukazawa, C., and Oku, T., Increasing the conformational stability by replacement of heme axial ligand in *c*-type cytochrome. *FEBS Lett.*, **531**, 543–547 (2002).
8) Lange, C., Hervás, M., and De la Rosa, M. A., Analysis of the stability of cytochrome c_6 with an improved stopped-flow protocol. *Biochem. Biophys. Res. Commun.*, **310**, 215–221 (2003).
9) Pettigrew, G. W., and Moore, G. R., "Cytochromes *c*: Evolutionary, Structural and Physicochemical Aspects," Springer, Berlin, pp. 161–170 (1990).
10) Otwinowski, Z., and Minor, W., Processing of X-ray diffraction data collected in oscillation mode. *Methods Enzymol.*, **276**, 307–326 (1997).
11) Collaborative Computational Project, Number 4, The CCP4 suite: programs for protein crystallography. *Acta Crystallogr. D*, **50**, 760–763 (1994).
12) Yamada, S., Park, S.-Y., Shimizu, H., Koshizuka, Y., Kadokura, K., Satoh, T., Suruga, K., Ogawa, M., Isogai, Y., Nishio, T., Shiro, Y., and Oku, T., Structure of cytochrome c_6 from the red alga *Porphyra yezoensis* at 1.57 Å resolution. *Acta Crystallogr. D*, **56**, 1577–1582 (2000).
13) Emsly, P., and Cowtan, K., Coot: model-building tools for molecular graphics. *Acta Crystallogr. D*, **60**, 2126–2132 (2004).
14) Kerfeld, C. A., Anwar, H. P., Interrante, R., Merchant, S., and Yeates, T. O., The structure of chloroplast cytochrome c_6 at 1.9 Å resolution: evidence for functional oligomerization. *J. Mol. Biol.*, **250**, 627–647 (1995).
15) Sawaya, M. R., Krogmann, D. W., Serag, A., Ho, K. K., Yeates, T. O., and Kerfeld, C. A., Structures of cytochrome *c*-549 and cytochrome c_6 from the cyanobacterium *Arthrospira maxima*. *Biochemistry*, **40**, 9215–9225 (2001).
16) Nakamura, H., Roles of electrostatic interaction in proteins. *Q. Rev. Biophys.*, **29**, 1–90 (1996).
17) Monera, O. D., Kay, C. M., and Hodges, R. S., Protein denaturation with guanidine hydrochloride or urea provides a different estimate of stability depending on the contributions of electrostatic interactions. *Protein Sci.*, **3**, 1984–1991 (1994).

Available online at www.sciencedirect.com
ScienceDirect
Bioorganic & Medicinal Chemistry Letters 18 (2008) 120–123
Bioorganic & Medicinal Chemistry Letters

(2*S*,2′*R*)-Analogue of LG190178 is a major active isomer

Wataru Hakamata,[a] Yukiko Sato,[a] Haruhiro Okuda,[a] Shinobu Honzawa,[b] Nozomi Saito,[b] Seishi Kishimoto,[b] Atsushi Yamashita,[b] Takayuki Sugiura,[b] Atsushi Kittaka[b] and Masaaki Kurihara[a,*]

[a]*Division of Organic Chemistry, National Institute of Health Sciences, Kamiyoga, Setagaya-ku, Tokyo 158-8501, Japan*
[b]*Faculty of Pharmaceutical Sciences, Teikyo University, Sagamiko, Kanagawa 199-0195, Japan*

Received 27 June 2007; revised 17 October 2007; accepted 1 November 2007
Available online 5 November 2007

Abstract—Vitamin D receptor (VDR) ligands are therapeutic agents for the treatment of psoriasis, osteoporosis, and secondary hyperparathyroidism. VDR ligands also show immense potential as therapeutic agents for autoimmune diseases and cancers of the skin, prostate, colon, and breast as well as leukemia. LG190178 is a novel non-secosteroidal ligand for VDR. We synthesized and evaluated stereoisomers of LG190178 and found that only an (2*S*,2′*R*)-analogue of LG190178 (YR301) had strong activity.

The active form of vitamin D_3, 1α,25-dihydroxyvitamin D_3 (1α,25-$(OH)_2D_3$), is not only a regulator of calcium homeostasis and bone development and remodeling but also a potent differentiator of leukemic cells. 1α,25-$(OH)_2D_3$ and its synthetic analogues exert these effects by binding to the vitamin D receptor (VDR) which belongs to the steroid/thyroid hormone nuclear receptor superfamily. The X-ray crystal structure of the ligand binding domain (LBD) of VDR with 1α,25-dihydroxyvitamin D_3 was determined by Moras et al. in 2000 and the binding mode between ligands and LBD-VDR was revealed.[1] This enables the design of VDR ligands by structure-based drug design. We have also designed secosteroidal analogues[2] (Fig. 1).

Recently, non-secosteroidal ligands for VDR have been an attractive target for the development of new therapeutics.[3] LG190178 is the first novel non-secosteroidal ligand, with potential as therapeutic for cancer, leukemia, and psoriasis with less calcium mobilization side effects than are associated with secosteroidal 1α,25-$(OH)_2D_3$ analogues,[4] however, LG190178 includes four stereoisomers.[5] We calculated to make ducking model of four isomers and VDR, respectively,[6] and the results are summarized in Figure 2 and Table 1. The (2*S*,2′*R*)-isomer model was the most stable. There were hydrogen bonds between 2-OH and Arg-274, Ser-237 and between 2′-OH and His-305, His-397. (2*S*)-Isomers ((2*S*,2′*S*) and (2*S*,2′*R*)) are expected to be more important than (2*R*)-isomers.

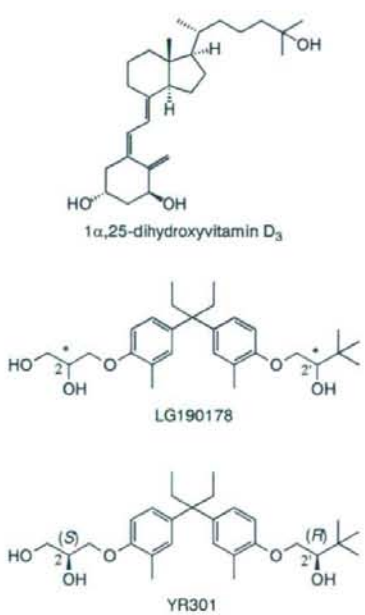

Figure 1. Structure of 1α,25-dihydroxyvitamin D_3, LG190178, and YR301.

Keywords: Vitamin D receptor; Non-secosteroidal ligand; (2*S*,2′*R*)-LG190178; YR301.
* Corresponding author. E-mail: masaaki@nihs.go.jp

0960-894X/$ - see front matter
doi:10.1016/j.bmcl.2007.11.007

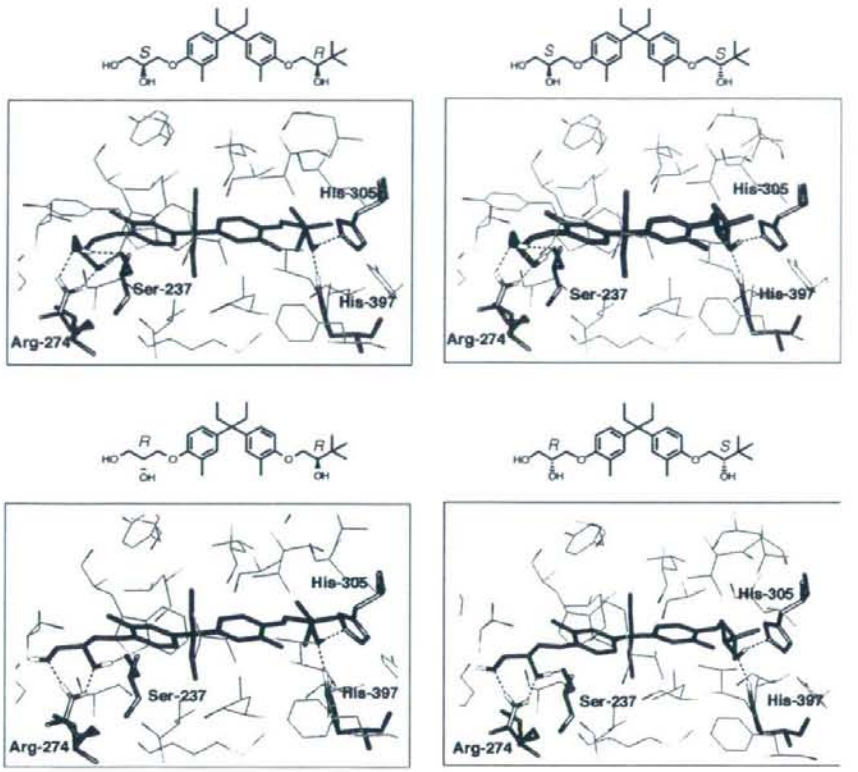

Figure 2. Modeled structure of stereoisomers of LG190178 bound to VDR.

Table 1. Difference of potential energy of docking modeling of four isomers and VDR

Model	AE (kcal/mol)
I (2*S*,2′*R*)	0
II (2*S*,2′*S*)	+1.87
III (2*R*,2*R*)	+3.56
IV (2*R*,2′*S*)	+4.94

We synthesized (2*S*)-LG190178 and (2*R*)-LG190178. The synthetic routes of (2*S*)-isomers and (2*R*)-isomers are shown in Scheme 1. The 2-position asymmetric center was constructed using optically active glycidols. (2*S*)-Analogues and (2*R*)-analogues were analyzed by HPLC with a chiral column (CHIRALPAK IA, solvent: hexane/EtOH 9:1). HPLC charts are shown in Figure 3. The four isomers are YR301, YR302, YR303, and YR304, respectively. To determine the stereochemistry of the 2′-position, we synthesized the (2*S*,2′*R*)-isomer from (*R*)-diol **6**. (*R*)-1-(Benzyloxy)-3,3-dimethylbutan-2-ol **5** was separated using HPLC with a chiral column (CHIRALPAK IA, DAICEL; solvent: hexane/EtOH 9:1) and hydrogenated in the presence of $Pd(OH)_2/C$ to afford compound **6** ($[\alpha]_D^{25}$ −31.6 (*c* = 1.00, methanol)) in 70% yield. Absolute configuration of **6** was determined by comparing the optical rotation of **6** with that of the literature.[7] Scheme 3 shows the synthesis of the (2*S*,2′*R*)-isomers from (*R*)-diol **6**. Then YR301 was determined to be the (2*S*,2′*R*)-isomer. Using the same procedures YR302, 303, and 304 were determined to be (2*S*,2′*S*)-isomer, (2*R*,2′*R*)-isomer, and (2*R*,2′*S*)-isomer, respectively (Scheme 2).

Isomers were examined for transcriptional assays and VDR affinity. The results are summarized in Table 2. (2*S*,2′*R*)-Isomer (YR301) exhibited potent transcriptional activity, comparable to natural ligand 1α, 25-$(OH)_2D_3$. Moreover, in the cases of human colon carcinoma cell, YR301 exhibited stronger activities than 1α,25-$(OH)_2D_3$. (2*S*,2′*S*)- and (2*R*,2′*R*)-isomers, diastereomers of (2*S*,2′*R*), decreased the activity by two orders of magnitude, compared with (2*S*,2′*R*)-isomer (YR301). (2*R*,2′*S*)-Isomer, the enantiomer of (2*S*,2′*R*) exhibited the weakest activity. It is very interesting that only YR301 showed strong activity. Figure 4 shows an overlay of the X-ray structure of 1α,25-$(OH)_2D_3$ and modeled structure of (2*S*,2′*R*)-isomer (YR301) in LBD of VDR. YR301 is well overlapped with 1α,25-$(OH)_2D_3$, especially with the hydrophobic region, but YR301 is not expected to be H-bonded to Tyr-143 and Ser-278, which are H-bonded to 1α,25-$(OH)_2D_3$. It is important to remember that considering H-bonds to Tyr-143 and Ser-278 is important in the design of new ligands.

In summary, we revealed that YR301, an (2*S*,2′*R*)-analogue of LG190178, was a major active isomer. YR301

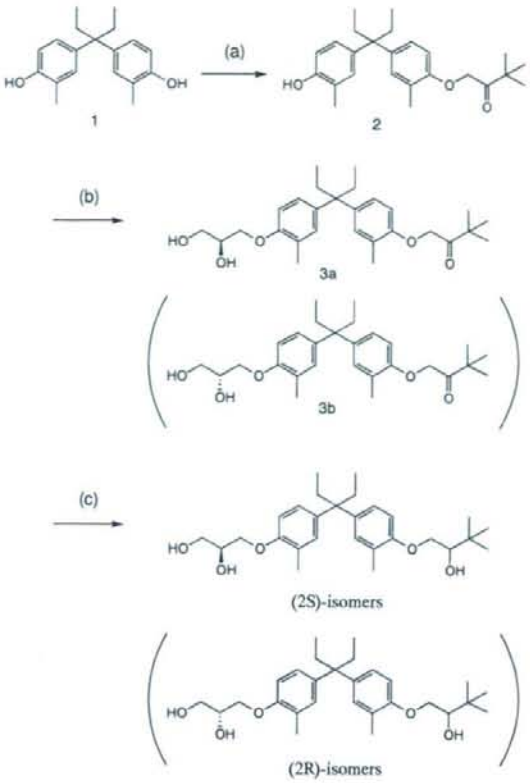

Scheme 1. Reagents and conditions: (a) $ClCH_2CO'Bu$, NaH, DMF, 80 °C, 12 h, 40%; (b) (*S*)-glycidol (or (*R*)-glycidol), NaH, DMF, 80 °C, 3 h, 59%; (c) $NaBH_4$, MeOH, rt, 2 h, 89%.

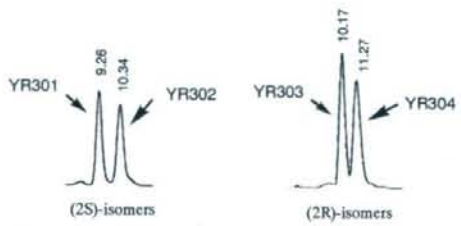

Figure 3. HPLC chart.

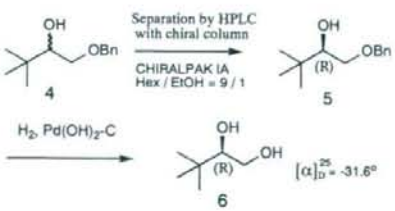

Scheme 2. Separation and determination of chiral.

exhibited potent biological activity, comparable to natural ligand $1\alpha,25\text{-}(OH)_2D_3$. Non-secosteroidal ligands for VDR are novel candidates for therapeutic agents.

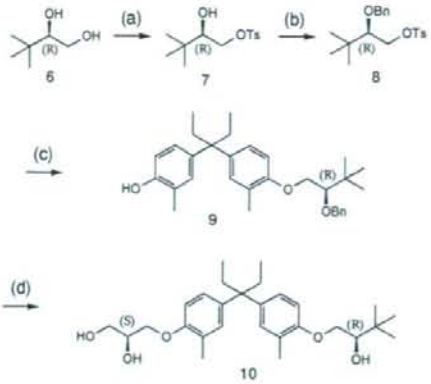

Scheme 3. Reagents and conditions: (a) TsCl, C_5H_5N, CH_2Cl_2, rt, 19 h, 52%; (b) benzy trichloroacetimidate, TMSOTf, DMF, rt, 5 h, 72%; (c) **1**, NaH, DMF, rt, 1 h, 32%; (d) (*S*)-glycidol, NaH, DMF, 80 °C, 3 h, 43%; H_2, $Pd(OH)_2/C$, rt, 24 h, 93 h.

Table 2. Biological activities for transcriptional assays and VDR affinity

Compound	Transcription EC_{50} (nM)			VDR affinity
	HOS/SF[a]	HOS/5% FCS[b]	Caco-2/5% FCS[c]	
$1\alpha,25(OH)_2D_3$	0.0106	0.555	3.52	100
YR301 (2*S*,2′*R*)	0.0396	0.79	1.80	28.3
YR302 (2*S*,2′*S*)	1.66	9.9	21.1	0.831
YR303 (2*R*,2′*R*)	4.68	16.8	22.1	0.482
YR304 (2*R*,2′*S*)	15.6	83.2	131.4	0.112

[a] Human osteosarcoma cell, serum free.
[b] Human osteosarcoma cell, 5% fetal calf serum.
[c] Human colon carcinoma cell, 5% fetal calf serum.

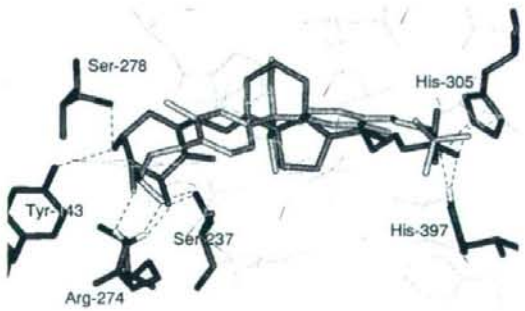

Figure 4. Overlay of the X-ray structure of $1\alpha,25\text{-}(OH)_2D_3$ and modeled structure of YR301 in VDR. $1\alpha,25\text{-}(OH)_2D_3$ and YR301 are shown in orange and green, respectively. Hydrogen bonds are drawn as dotted lines.

Acknowledgments

This work was supported in part by the Budget for Nuclear Research of the Ministry of Education, Culture, Sports, Science, and Technology, based on the screening and counseling by the Atomic Energy Commission and by a Grant-in-Aid for Scientific Research (C) from the Japan Society for the Promotion of Science.

References and notes

1. Rochel, N.; Wurtz, J. M.; Mitschler, A.; Klaholz, B.; Moras, D. *Mol. Cell.* **2000**, *5*, 173.
2. (a) Kittaka, A.; Suhara, Y.; Takayanagi, H.; Fujishima, T.; Kurihara, M.; Takayama, H. *Org. Lett.* **2000**, *2*, 2619; (b) Konno, K.; Fujishima, T.; Maki, S.; Liu, Z.; Miura, D.; Chokki, M.; Ishizuka, S.; Yamaguchi, K.; Kan, Y.; Kurihara, M.; Miyata, N.; Smith, C.; DeLuca, H. F.; Takayama, H. *J. Med. Chem.* **2000**, *43*, 4247; (c) Fujishima, T.; Konno, K.; Nakagawa, K.; Tanaka, M.; Okano, T.; Kurihara, M.; Miyata, N.; Takayama, H. *Chem. Biol.* **2001**, *8*, 1011; (d) Suhara, S.; Nihei, K.; Kurihara, M.; Kittaka, A.; Fujishima, T.; Konno, K.; Miyata, N.; Takayama, H. *J. Org. Chem.* **2001**, *66*, 8760; (e) Suhara, Y.; Kittaka, A.; Ono, K.; Kurihara, M.; Fujishima, T.; Yoshida, A.; Takayama, H. *Bioorg. Med. Chem. Lett.* **2002**, *12*, 3533; (f) Kittaka, A.; Kurihara, M.; Peleg, S.; Suhara, Y.; Takayama, H. *Chem. Pharm. Bull.* **2003**, *51*, 357; (g) Honzawa, S.; Suhara, Y.; Nihei, K.; Saito, N.; Kishimoto, S.; Fujishima, T.; Kurihara, M.; Sugiura, T.; Waku, K.; Takayama, H.; Kittaka, A. *Bioorg. Med. Chem. Lett.* **2003**, *13*, 3503; (h) Saito, N.; Suhara, Y.; Kurihara, M.; Fujishima, T.; Honzawa, S.; Takayanagi, H.; Kozono, T.; Matsumoto, M.; Ohmori, M.; Miyata, N.; Takayama, H.; Kittaka, A. *J. Org. Chem.* **2004**, *69*, 7463; (i) Kurihara, M.; Rouf, A. S. S.; Kansui, H.; Kagechika, H.; Okuda, H.; Miyata, N. *Bioorg. Med. Chem. Lett.* **2004**, *14*, 4131; (j) Honzawa, S.; Hirasaka, K.; Yamamoto, Y.; Peleg, S.; Fujishima, T.; Kurihara, M.; Saito, N.; Kishimoto, S.; Sugiura, T.; Waku, K.; Takayama, H.; Kittaka, A. *Tetrahedron* **2005**, *61*, 11253.
3. (a) Swann, S. L.; Bergh, J.; Farach-Carson, M. C.; Ocasio, C. A.; Koh, J. T. *J. Am. Chem. Soc.* **2002**, *124*, 13795; (b) Perakyla, M.; Malinen, M.; Herzig, K. H.; Carlberg, C. *Mol. Endocrinol.* **2005**, *19*, 2060; (c) Hosoda, S.; Tanatani, A.; Wakabayashi, K.; Nakano, Y.; Miyachi, H.; Nagasawa, K.; Hashimoto, Y. *Bioorg. Med. Chem. Lett.* **2005**, *15*, 4327; (d) Ma, Y.; Khalifa, B.; Yee, Y. K.; Lu, J.; Memezawa, A.; Savkur, R. S.; Yamamoto, Y.; Chintalacharuvu, S. R.; Yamaoka, K.; Stayrook, K. R.; Bramlett, K. S.; Zeng, Q. Q.; Chandrasekhar, S.; Yu, X. P.; Linebarger, J. H.; Iturria, S. J.; Burris, T. P.; Kato, S.; Chin, W. W.; Nagpal, S. *J. Clin. Invest.* **2006**, *116*, 892.
4. (a) Boehm, M. F.; Fitzgerald, P.; Zou, A.; Elgort, M. G.; Bischoff, E. D.; Mere, L.; Mais, D. E.; Bissonnette, R. P.; Heyman, R. A.; Nadzan, A. M.; Reichman, M.; Allegretto, E. A. *Chem. Biol.* **1999**, *6*, 265; (b) Polek, T. C.; Murthy, S.; Blutt, S. E.; Boehm, M. F.; Zou, A.; Weigel, N. L.; Allegretto, E. A. *Prostate* **2001**, *49*, 224.
5. Hashimoto's group reported bio-activities of stereoisomers of LG190178. Hosoda, S.; Tanatani, A.; Wakabayashi, K.; Makishima, M.; Imai, K.; Miyachi, H.; Nagasawa, K.; Hashimoto, Y. *Bioorg. Med. Chem.* **2006**, *14*, 5489.
6. A docking model of ligands bound to VDR (1DB1) was constructed by conformational search by MacroModel (ver. 8.1). AMBER* was used as force field. Differences of potential energy are estimated by molecular mechanics calculation.
7. William, A. N.; Richard, L. H. *J. Am. Chem. Soc.* **1994**, *116*, 6142.

J. Appl. Glycosci., 55, 157–164 (2008)

Proceedings of the Symposium on Amylases and Related Enzymes, 2007

Purification, Characterization and Cloning of *Vibrio parahaemolyticus* Chitinolytic Enzymes and Application to Oligosaccharide Production

(Received November 28, 2007; Accepted January 25, 2008)

Kazunari Kadokura,[1] Yusuke Sakamoto,[1] Akiko Rokutani,[1] Takanori Ikegami,[1] Takako Hirano,[1] Mahiro Yamamoto,[1] Kaori Saito,[1] Wataru Hakamata,[1] Shiro Itoi,[2] Haruo Sugita,[2] Tadatake Oku[1] and Toshiyuki Nishio[1,*]

[1]*Department of Biological Chemistry, and*
[2]*Department of Marine Sciences and Resources, College of Bioresource Sciences, Nihon University*
(1866, Kameino, Fujisawa, Kanagawa 252–8510, Japan)

Abstract: Chitinase (*Pa*-Chi) and chitin oligosaccharide deacetylase (*Pa*-COD) are involved in the production of a heterodisaccharide, β-D-*N*-acetylglucosaminyl-(1,4)-D-glucosamine (GlcNAc-GlcN). These enzymes were recovered from the supernatant of *Vibrio parahaemolyticus* KN1699 cell culture and purified and characterized. For each enzyme, an ORF encoding gene and its signal sequence were cloned from genomic DNA of strain KN1699. In addition, the expression plasmid was constructed for each enzyme gene and inserted into *Escherichia coli* cells, and recombinant *Pa*-Chi and *Pa*-COD (*Pa*-rChi and *Pa*-rCOD) were secreted into the culture medium with the aid of signal peptides. Di-*N*-acetylchitobiose [$(GlcNAc)_2$] was produced in 60% (w/w) yield by cultivating the *Pa*-rChi-secreting *E. coli* cells in 2% (w/v) β-chitin-containing medium. Moreover, GlcNAc-GlcN was produced in high yield by treating $(GlcNAc)_2$ with the culture supernatant of *Pa*-rCOD-secreting *E. coli* cells.

Key words: *Vibrio parahaemolyticus*, chitinase, chitin oligosaccharide deacetylase, heterodisaccharide, recombinant enzyme

Oligosaccharides can exhibit physiologically useful functions. Many of these oligosaccharides are prepared by enzymatic degradation of biomass polysaccharides, or by enzymatic conversion of oligosaccharides produced by higher plants. New oligosaccharides with potential therapeutic activities are currently being developed; the physiological properties of oligosaccharides obtained by the hydrolysis of chitin, a β-(1,4) polymer of *N*-acetyl-D-glucosamine (GlcNAc), are of particular interest. Studies have reported that hexa-*N*-acetylchitohexaose, $(GlcNAc)_6$, exhibits antitumor[1–3] and antimicrobial activity[4,5] in mice by enhancing the immunological defense system. These findings have focused attention on GlcNAc and $(GlcNAc)_6$ as potential agents for arthritis therapy and immunotherapy, respectively, and have raised the possibility that chitin oligosaccharides could have physiologically useful functions. Generally, GlcNAc and chitin oligosaccharides are obtained by hydrolysis of chitin using strong acid. Chitin, one of the most abundant of all biomass polysaccharides, is the major component of the shells of crustaceans such as crab and shrimp, the exoskeletons of insects, and the cell walls of fungi. The hydrolysis of this biomass polysaccharide by enzymes possessing high product specificity would be more efficient than acid hydrolysis for the production of specific oligosaccharides. Various enzymes involved in chitin hydrolysis [*e.g.*, chitinase (EC 3.2.1.14), β-*N*-acetylhexosaminidase (EC 3.2.1.52), chitin deacetylase (EC 3.5.1.41), and chitin oligosaccharide deacetylase (EC 3.5.1.—)] have been identified. Chitinase catalyzes the degradation of water-insoluble chitin into water-soluble chitin oligosaccharides through hydrolysis. A number of chitinases have been isolated from bacteria and their properties investigated.[6] In addition, genes encoding a variety of chitinases have been cloned. Based on their amino acid sequences, these chitinases are classified as belonging to either glycoside hydrolase (GH) family 18 or 19 (http://afmb.cnrs-mrs.fr/CAZY/). β-*N*-Acetylhexosaminidase catalyzes hydrolysis of chitin oligosaccharides to release the monosaccharide GlcNAc. Enzymes from various sources have been classified in three GH families: 3, 20 (the main family), and 84. Microbial β-*N*-acetylhexosaminidases have been reviewed.[7] Chitin deacetylase and chitin oligosaccharide deacetylase are involved in hydrolysis of the acetamide group of the GlcNAc residue of chitin and chitin oligosaccharides.[8] Both enzymes, isolated from various sources, are classified as belonging to carbohydrate esterase (CE) family 4 (http://afmb.cnrs-mrs.fr/CAZY/). Several microbial chitin deacetylases and chitin oligosaccharide deacetylases have been isolated and characterized.[9–13] Previously, high-yield production of di-*N*-acetylchitobiose, $(GlcNAc)_2$, had been accomplished by cultivating the *exo*-type chitinase-producing marine bacterium, *Vibrio anguillarum* E-383a, in a medium containing colloidal chitin.[14]

To obtain the enzymes that produce specific oligosaccharides from chitin effectively, we screened chitin-degrading bacteria isolated from dry beach soil and from the contents of marine fish intestines. Enzymes were screened by observing the formation of clear zones around

* Corresponding author (Tel. +81–466–84–3951, Fax. +81–466–84–3951, E-mail: nishio@brs.nihon-u.ac.jp).

colonies on colloidal chitin-agar plates. A number of bacterial strains having chitin-degrading activity were isolated from Yatsu dry beach (Narashino, Chiba Prefecture, Japan). We chose one type of bacterium (KN1699) from those isolated, through tests involving both chitin decomposition and oligosaccharide production. The bacterium isolated was identified as *V. parahaemolyticus* from its morphological and physiological characteristics and nucleotide sequence encoding its 16S rDNA.[15] Here, we describe the results of oligosaccharide production by extracellular chitin-degrading enzymes of strain KN1699, as well as the purification and characterization of the enzymes, cloning of enzyme genes, preparation of recombinant enzyme-secreting *Escherichia coli* cells, and oligosaccharide production using transformed *E. coli* cells and the recombinant enzyme.

Oligosaccharide production by extracellular chitin-degrading enzymes of V. parahaemolyticus KN1699.[15]

The oligosaccharide produced by the action of crude enzyme (prepared from the supernatant of *V. parahaemolyticus* KN1699 cultures) on β-chitin was analyzed using silica gel thin layer chromatography (TLC). When phosphomolybdic acid reagent was used to visualize the oligosaccharide, TLC of the reaction mixture indicated a single product (Fig. 1a). Ninhydrin reagent also visualized this product, suggesting the product is an oligosaccharide possessing a free amino group. Although the mobility of this compound corresponded to that of chitobiose [$(GlcN)_2$], its structure needed confirmation. Therefore, the compound was purified and its structure analyzed by ESIMS and ^{1}H NMR. The data indicated that the compound produced from β-chitin by the action of crude enzyme, prepared from the supernatant of *V. parahaemolyticus* KN 1699 cultures, was β-D-*N*-acetylglucosaminyl-(1,4)-D-glucosamine (GlcNAc-GlcN) (Fig. 1b).

This heterodisaccharide appeared to be produced by the reactions of both chitinase and chitin oligosaccharide deacetylase, which were secreted into the culture medium by *V. parahaemolyticus* KN1699. To confirm this supposition, the enzymes were purified and their reactions examined.

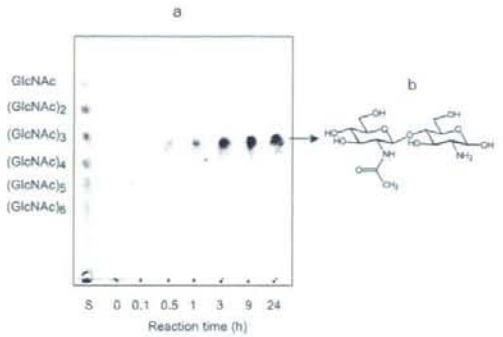

Fig. 1. Oligosaccharide produced from β-chitin by reaction of *V. parahaemolyticus* KN1699 extracellular chitinolytic enzyme.

The crude enzyme, which was prepared from supernatant of *V. parahaemolyticus* KN1699 culture, was added to 20 mM sodium phosphate buffer (pH 7.0) containing 0.5% (w/v) powdered β-chitin, then the mixture was incubated at 37°C with stirring. The reaction products of the various incubation times were subjected to silica gel thin layer chromatography (TLC) (Merck). After developing the TLC plates using 5:4:3 (v/v/v) *n*-butanol/methanol/16% aqueous ammonia as the mobile phase, the products were visualized using phosphomolybdic acid reagent.[15] The product was isolated from the reaction mixture by column chromatography using charcoal (Wako Pure Chemical) and Toyopearl HW-40F resin (Tosoh) columns, followed by structural analysis. a, TLC results; Lane S, *N*-acetylchitooligosaccharide standards; b, structure of reaction product.

Purification and characterization of extracellular enzymes involved in the production of the heterodisaccharide.[15]

Chitinase purification was accomplished in four steps from 1 L of culture fluid (Table 1). Each column chromatographic step produced a single peak showing chitinase activity. The purified enzyme gave a single band on both SDS-PAGE and native-PAGE (data not shown), indicating highly purified enzyme. The chitinase was purified 9.67-fold with 31.2% recovery of initial total activity. The spe-

Table 1. Purification of chitinolytic enzymes from culture supernatant of *V. parahaemolyticus* KN1699.

Purification step	Total activity (U)	Specific activity (U/mg of protein)	Yield (%)	Fold
Pa-Chi[a]				
$(NH_4)_2SO_4$ precipitation	34.4	0.24	100	1
DEAE-Toyopearl 650M (1st)	18.2	1.61	52.9	6.71
DEAE-Toyopearl 650M (2nd)	14.9	2.13	43.2	8.88
Toyopearl HW-55F	10.7	2.32	31.2	9.67
Pa-COD[b]				
$(NH_4)_2SO_4$ precipitation	1.95	0.01	100	1
DEAE-Sepharose FF	1.04	3.05	53.3	305
DEAE-Toyopearl 650M	0.76	9.50	39.0	950
Phenyl Sepharose HP	0.62	31.0	31.8	3100

Strain KN1699 was grown at 28°C for 16 h with shaking in half-strength artificial seawater containing 1% (w/v) peptone, 0.1% (w/v) yeast extract, and 0.5% (w/v) powdered α-chitin. The enzyme assay was performed according to a method described previously.[13] One unit of chitinase activity was defined as the amount of enzyme required to liberate reducing sugar equivalent to 1 μmol of GlcNAc per min under the assay conditions. One unit of chitin oligosaccharide deacetylase activity was defined as the amount of enzyme required to produce 1 μmol of GlcN residues per min under the assay conditions. [a]*Pa*-Chi was purified from 1 L of culture supernatant. [b]*Pa*-COD was purified from 2 L of culture supernatant.

cific activity of the purified enzyme toward powdered β-chitin was 2.32 U/mg protein. We named this chitinase *Pa*-Chi.

Chitin oligosaccharide deacetylase was purified in four steps from 2 L of culture fluid (Table 1). Each column chromatographic step produced a single peak possessing deacetylase activity. The purified enzyme gave a single band on both SDS-PAGE and native-PAGE (data not shown), indicating highly purified enzyme. Chitin oligosaccharide deacetylase was purified 3100-fold with 31.8% recovery of initial total activity. The specific activity of the purified enzyme toward $(GlcNAc)_2$ was 31 U/mg protein. Although the amount of deacetylase protein in the culture supernatant was very small, its specific activity was significantly higher than that of *Pa*-Chi. We named this chitin oligosaccharide deacetylase *Pa*-COD. The molecular masses of *Pa*-Chi and *Pa*-COD were estimated by SDS-PAGE to be 92 and 46 kDa, respectively, based on molecular mass standards. The *N*-terminal amino acid sequences of *Pa*-Chi and *Pa*-COD were APTAPSVDMY GSNNLQFSKIELAMET and QTDTKGTIYLTFDDGPI NASIDVINV, respectively. *Pa*-Chi and *Pa*-COD were most active at pH 8.0 and 8.5–9.0, respectively, and the optimum reaction temperature was 50–55°C for *Pa*-Chi and 45°C for *Pa*-COD.

The TLC mobility results indicate that $(GlcNAc)_2$ is the only oligosaccharide produced by the hydrolytic action of *Pa*-Chi on β-chitin (Fig. 2a-1). The product did not react with ninhydrin (Fig. 2a-2), indicating that *Pa*-Chi hydrolyzed β-chitin to $(GlcNAc)_2$. Reaction of *Pa*-Chi with $(GlcNAc)_6$ also gave only $(GlcNAc)_2$ as the final product (data not shown). The TLC results with *Pa*-COD indicated that this enzyme converts $(GlcNAc)_2$ to a saccharide that is more polar than $(GlcNAc)_2$ (Fig. 2b-1) and possesses a free amino group (Fig. 2b-2). The ^1H NMR analysis confirmed the structure of this product as GlcNAc-GlcN. *Pa*-COD was confirmed to possess the greatest substrate specificity for $(GlcNAc)_2$ out of the oligosaccharides examined. These results indicate that *Pa*-Chi is an *exo*-*N,N*-diacetylchitobiohydrolase-like enzyme and *Pa*-COD catalyzes the hydrolysis of the acetamide group of the reducing end GlcNAc residue of $(GlcNAc)_2$. The findings demonstrate that GlcNAc-GlcN is produced from chitin by the cooperative hydrolytic reactions of *Pa*-Chi and *Pa*-COD, both of which are present in the supernatant of *V. parahaemolyticus* KN1699 cultures.

Cloning of enzyme genes and expression of recombinant enzymes in the culture medium of Escherichia coli cells.[16,17]

The *N*-terminal amino acid sequences (26 residues) of both *Pa*-Chi and *Pa*-COD showed 100% identity with those estimated from the nucleotide sequences of the *V. parahaemolyticus* RIMD 2210633 putative genes of corresponding enzymes (GeneBank accession no.: chitinase; BA000032-55, chitin oligosaccharide deacetylase; BA 000031-2638). This suggests similarity in the nucleotide sequences in the vicinity of both the chitinase and chitin oligosaccharide deacetylase genes in *V. parahaemolyticus* KN1699 and RIMD 2210633 genomic DNA. Therefore, PCR forward and reverse primers for cloning *Pa*-Chi and *Pa*-COD genes were designed from upstream and downstream nucleotide sequences of putative chitinase and chitin oligosaccharide deacetylase genes in genomic DNA of strain RIMD2210633. After sub-cloning of the PCR products into the vector, their nucleotide sequences were analyzed. The ORF of *Pa*-Chi (GeneBank accession no.: AB 299855) consisting of 2544 bp and encoding 848 amino acid residues was found in the PCR product. The *N*-terminal sequence analysis of *Pa*-rChi showed that the signal sequence corresponds to the 21 *N*-terminal amino acids. The recombinant enzyme consisted of 827 amino acids, with a molecular weight of 88,001 Da. This molecular weight is consistent with that of purified *Pa*-Chi.[15] As expected, two motifs conserved in the catalytic regions of GH family 18 chitinases, S-x-G-G (amino acid no. 271–274) and x-D-x-x-D-x-D-x-E (amino acid no. 307–315) (E is a catalytic amino acid residue),[18] also were pre-

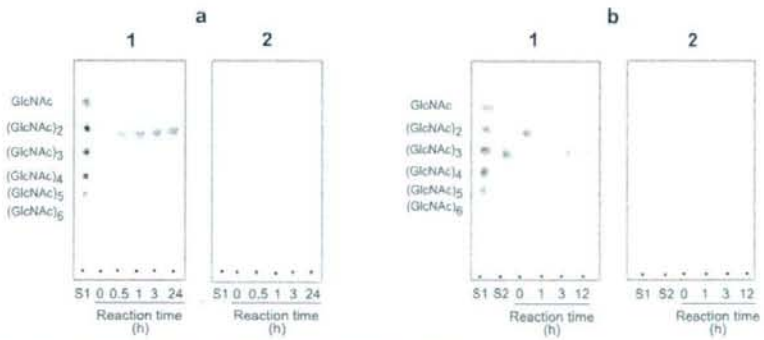

Fig. 2. TLC analysis of oligosaccharides produced by the reactions of purified enzymes.

Purified *Pa*-Chi (30 mU) was added to 1 mL of 20 mM sodium phosphate buffer (pH 7.0) containing 0.5% (w/v) of powdered β-chitin, then the mixture was incubated at 37°C with stirring. Purified *Pa*-COD (3.12 mU) was added to 80 μL of 20 mM sodium phosphate buffer (pH 7.0) buffer containing 0.5% of $(GlcNAc)_2$, then the mixture was incubated at 37°C. After developing the TLC plates containing the reaction products of various incubation times using 5:4:3 (v/v/v) *n*-butanol/methanol/16% aqueous ammonia as mobile phase, the products were visualized. TLC results of the reaction mixture with *Pa*-Chi are shown in a. TLC results of the reaction mixture with *Pa*-COD are shown in b. Reaction products on the TLC plates were visualized using the following reagents; a-1 and b-1, phosphomolybdic acid reagent; a-2 and b-2, ninhydrin reagent. Lane S1, *N*-acetylchitooligosaccharide standards; lane S2, GlcNAc-GlcN.

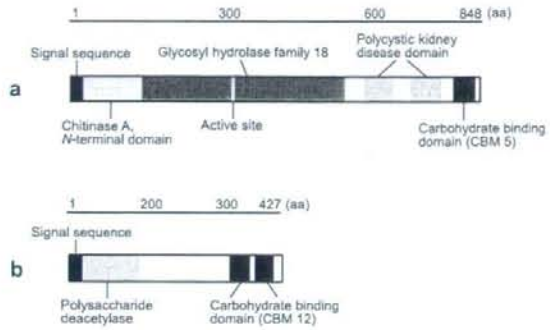

Fig. 3. Motifs of recombinant enzymes.

a, *Pa*-rChi; b, *Pa*-rCOD.

sent in *Pa*-rChi. The carbohydrate binding domain classified in carbohydrate binding module (CBM) family 5 (http://afmb.cnrs-mrs.fr/CAZY/) was observed in the *C*-terminal region (amino acid no. 797–839) of *Pa*-rChi. The motif of *Pa*-rChi is illustrated in Fig. 3a. The amino acid sequence of this recombinant enzyme was highly homologous to several GH family 18 chitinases from *Vibrionaceae* bacteria: 100% identity with *V. alginolyticus* H-8 ChiB[19] (GeneBank accession no. AJ292004), 99.8% identity with *V. parahaemolyticus* RIMD 2210633 Chi, 97% identity with *V. alginolyticus* 12G01 Chi (GeneBank accession no. AAPS01000021), and 93.1% identity with *V. carchariae* ChiA (GeneBank accession no. AF323180).[20] The ORF of *Pa*-COD (GeneBank accession no. AB 275387) consisting of 1281 bp was found in the PCR product, and encoded 427 amino acid residues. The *N*-terminal sequence analysis of *Pa*-rCOD showed that the signal sequence corresponds to the 22 *N*-terminal amino acids. The recombinant enzyme consisted of 405 amino acids, with a molecular weight of 44,715 Da. This value is in good agreement with that obtained by SDS-PAGE analysis of *Pa*-COD.[15] The carbohydrate-binding domain classified in CBM family 12 (http://afmb.cnrs-mrs.fr/CAZY/) was observed in the *C*-terminal region (amino acid no. 332–366, 381–415) of *Pa*-rCOD. The motif of this recombinant enzyme is illustrated in Fig. 3b. The amino acid sequence of *Pa*-rCOD showed high homology with those of CE family 4 chitin oligosaccharide deacetylases from *Vibrionaceae* bacteria. Three amino acids (290, 394 and 396) were different between *Pa*-rCOD and the putative deacetylase (405 amino acids) from *V. parahaemolyticus* RIMD2210633. Four amino acids (173, 290, 394 and 396) were different between *Pa*-rCOD and the deacetylase from *V. alginolyticus* H-8 (DA1, 405 amino acids; GeneBank accession number AJ292005).[21] Moreover, *Pa*-rCOD showed 83% identity with the putative deacetylase from *V. vulnificus* CMC-6 and *V. vulnificus* YJ016, and 82% identity with the putative deacetylase from *V. cholerae* E1 Tor N16961.

The ORF containing the ribosome-binding sequence, the signal sequence, and each enzyme gene was amplified by PCR and inserted into the pET-21(+) vector to make expression plasmid (*Pa*-rChi expression plasmid, pVP-Chi; *Pa*-rCOD expression plasmid, pVP-COD2) (Figs. 4a and 4b), and then *E. coli* BL21(DE3) cells were transformed with each plasmid. The *E. coli* cells harboring the plasmid were cultivated and production of recombinant enzyme was induced by addition of IPTG. Figure 5a shows the time course of chitinase activity in both lysates and the culture medium of *E. coli* cells harboring pVP-Chi. Time courses of deacetylase activity in both lysates and the culture medium of *E. coli* cells harboring pVP-COD2 are shown in Fig. 5c. Addition of IPTG initiated production of recombinant enzyme in *E. coli* cells, while its secretion into the culture medium increased gradually. Chitinase activity in the medium exceeded that in the *E. coli* lysates after 7 h of cultivation. After 12 h of cultivation, total deacetylase activity in the culture medium peaked at the same level as that in *E. coli* lysates. Figures

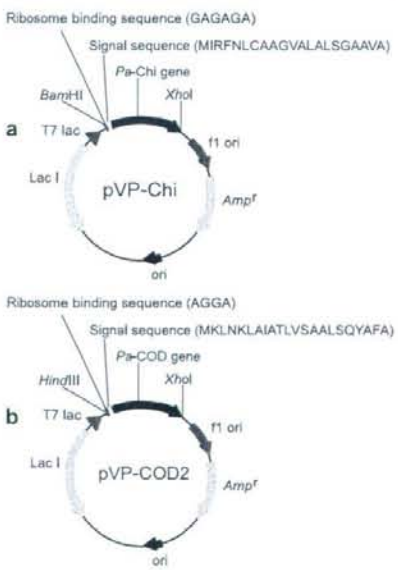

Fig. 4. Plasmids for expression of recombinant enzymes.

An ORF containing the ribosome-binding sequence, signal sequence, and enzyme gene was amplified with different restriction enzyme sites by PCR. After the PCR product was isolated from agarose gel slice and digested with two corresponding restriction enzymes, the resulting DNA fragment was ligated into pET-21(+) (Novagen), which was digested by these restriction enzymes to yield the following expression plasmids: a, pVP-Chi for *Pa*-rChi production; b, pVP-COD2 for *Pa*-rCOD production.

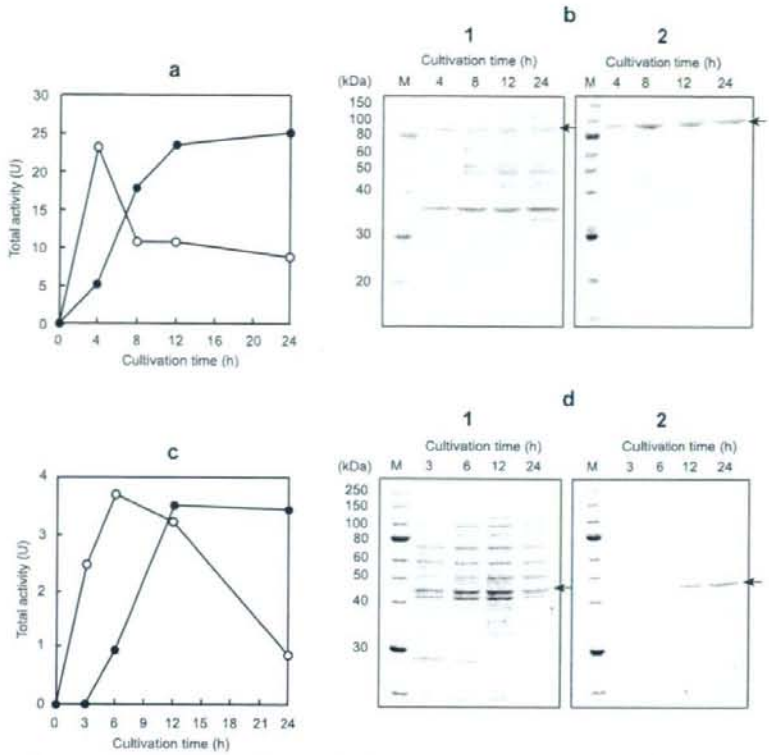

Fig. 5. Time course of recombinant enzyme production after addition of IPTG to the transformed *E. coli* culture.

Aliquots (7 mL) of transformed *E. coli* culture broth were withdrawn at the chosen time points and centrifuged to harvest the cells and obtain the culture supernatant. Pelleted transformed *E. coli* cells were suspended in 7 mL of phosphate buffered saline, and the cell membranes were disrupted by sonication to produce the cell lysate. The culture supernatants obtained were dialyzed against 20 mM of sodium phosphate buffer (pH 7.0). a, *Pa*-rChi production; ○, total chitinase activity in lysate of *E. coli* cells (calculated as amount of activity in the cells harvested from 100 mL of culture broth); ●, total chitinase activity (calculated as an amount of activity in 100 mL of culture supernatant); b, SDS-PAGE results with *Pa*-rChi in cell lysate (1) and culture supernatant (2) of transformed *E. coli*; c, *Pa*-rCOD production; ○, total chitin oligosaccharide deacetylase activity in lysate of *E. coli* cells harvested from 7 mL of culture broth; ●, total chitin oligosaccharide deacetylase activity in 7 mL of culture supernatant; d, SDS-PAGE results with *Pa*-rCOD in cell lysate (1) and culture supernatant (2) of transformed *E. coli*. Lane M shows molecular mass standards (Promega). The arrows indicate *Pa*-rChi and *Pa*-rCOD, respectively.

5b-1 and -2 show SDS-PAGE results of the time course of the *Pa*-rChi production in both transformed *E. coli* cells and their culture medium. The SDS-PAGE results showing time courses of the production of *Pa*-rCOD in both transformed *E. coli* cells and their culture medium are shown in Figs. 5d-1 and -2. In both culture media, the proteins with molecular masses of approximately 90 kDa and 45 kDa were confirmed as the main products, while other proteins secreted by the transformed *E. coli* cells were present in very low concentrations. Chitinase activity was eight-fold greater in the *E. coli* culture medium than in *V. parahaemolyticus* KN1699 culture medium. The amount of deacetylase activity in the *E. coli* culture medium was 150 times greater than in the culture medium of the strain KN1699. The *N*-terminal amino acid sequence of *Pa*-rChi and *Pa*-rCOD were same as the corresponding wild-type enzymes, indicating that the signal peptide regions of the expression products were removed as the proteins crossed the *E. coli* cell membrane. Substrate specificities and hydrolysis products of both recombinant enzymes were the same as those of corresponding wild-type enzymes.

Production of oligosaccharide from chitin by transformed E. coli cells and recombinant enzyme.

GlcNAc-GlcN, produced from chitin by cooperative reactions of both *Pa*-Chi and *Pa*-COD, is a unique oligosaccharide. Similar to other rare oligosaccharides, GlcNAc-GlcN is likely to possess physiologically useful activity. Gram-scale production of this heterodisaccharide was attempted to obtain material for function studies. However, the production of both *Pa*-Chi and *Pa*-COD from *V. parahaemolyticus* KN1699 was extremely low. Therefore, we decided to produce this heterodisaccharide using overproduced recombinant enzymes of *Pa*-Chi and *Pa*-COD (*Pa*-rChi and *Pa*-rCOD). To make GlcNAc-GlcN using *Pa*-rCOD, it is necessary to obtain $(GlcNAc)_2$ through hydrolysis of chitin by *Pa*-rChi. As reported by Takiguchi and Shimahara,[14] production of chitin oligosaccharides by fermentation using chitinase-secreting microorganisms is convenient because the enzyme does not need to be extracted from the culture supernatant, and the

hydrolytic reaction can be performed effectively due to continuous production and secretion of the enzyme. Therefore, for the production of $(GlcNAc)_2$ from chitin, we performed fermentation using *Pa*-rChi-secreting *E. coli* cells. Evidence exists that addition of chitin to the culture medium is effective for recombinant chitinase production by transformed *E. coli* cells.[22] Therefore, we investigated *Pa*-rChi production by *E. coli* cells harboring pVP-Chi in LB medium containing powdered chitin (Fig. 6a). Although the addition of IPTG into the culture medium accelerated production of recombinant enzyme from an early stage, remarkable production of the enzyme began after 2 days of cultivation in the medium containing powdered chitin. After cultivation for 4 days, the amount of chitinase activity in the culture medium containing powdered chitin was 4-fold greater than in culture medium containing IPTG. SDS-PAGE results of *Pa*-rChi production in both culture supernatants corresponded to activity (Fig. 6b). The reason why addition of chitin into culture medium induces production of recombinant chitinase by transformed *E. coli* cells is not well understood. However, the phenomenon is useful for the production of $(GlcNAc)_2$ from chitin by fermentation using *E. coli* cells harboring pVP-Chi. By cultivating transformed *E. coli* cells in LB medium containing 50 μg/mL ampicillin and 2% (w/v) powdered β-chitin, $(GlcNAc)_2$ accumulation in the broth reached a maximum on the third day of culture, with a stoichiometric yield of 60% (w/w). Continued culture caused a rapid decrease in disaccharide concentration in the broth. In contrast, results of chitinase activity assays and SDS-PAGE analysis using culture supernatant at each culture time (Figs. 5a, b) confirmed that the cumulative amount of *Pa*-rChi increased throughout the culture period. Many strains of *E. coli* are known to uptake and metabolize $(GlcNAc)_2$.[23] This suggests that production and consumption of $(GlcNAc)_2$ by *Pa*-rChi and *E. coli* cells occurs synchronically during the culture period. Almost all of the β-chitin added appears to be converted to $(GlcNAc)_2$ by culturing for 3 days. A rapid decrease in $(GlcNAc)_2$ after 3 days of culture may be due to both disappearance of substrate chitin and consumption of the disaccharide by *E. coli* cells. Fermentation using *Pa*-rChi-secreting *E. coli* cells and powdered β-chitin produced $(GlcNAc)_2$ in high yield, similar to fermentation using *V. anguillarum* E-383 a and colloidal chitin.[14] Addition of 25 units of *Pa*-rCOD, prepared from the culture supernatant of *E. coli* cells harboring pVP-COD2, to 50 mL of 20 mM sodium phosphate buffer (pH 7.0) containing 0.5 g $(GlcNAc)_2$ at 37°C produced GlcNAc-GlcN in 89% (mol/mol) yield after 2 days. The methods and results for production of this heterodisaccharide from chitin are illustrated in Fig. 7.

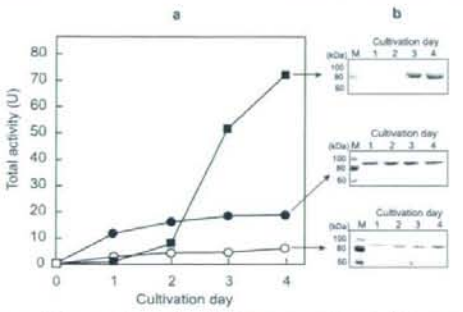

Fig. 6. Influence of powdered chitin on recombinant chitinase production by transformed *E. coli*.

IPTG and powdered β-chitin were added into different cultures of transformed *E. coli* at final concentrations of 1 mM and 2% (w/v), respectively, and the cultures were incubated with shaking for an additional 4 days. Aliquots of culture broth were withdrawn at the chosen time points and centrifuged to obtain culture supernatants. These culture supernatants were dialyzed against 20 mM of sodium phosphate buffer (pH 7.0). a, *Pa*-rChi production; ○, total chitinase activity in the supernatant from culture using LB medium; ●, total chitinase activity in the supernatant from culture using LB medium containing IPTG; ■, total chitinase activity in the supernatant from culture using LB medium containing powdered β-chitin; b, SDS-PAGE results with *Pa*-rChi for each culture supernatant.

Further studies are underway using the prepared GlcNAc-GlcN to investigate its physiological functions.

This study was supported in part by a grant from Nihon University and by a "High-Tech Research Center Project" of the Ministry of Education, Science, Sports and Culture of Japan to promote advanced scientific research.

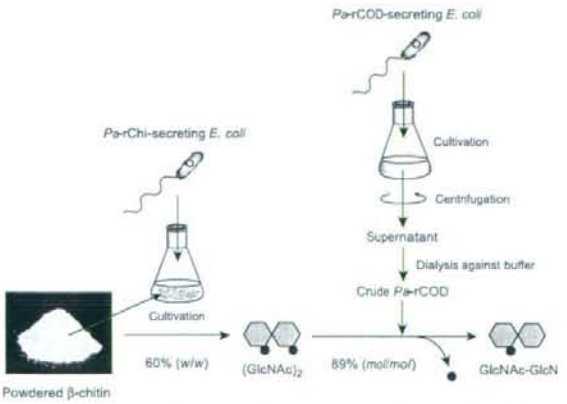

Fig. 7. Outline of the oligosaccharide production from powdered chitin.

REFERENCES

1) K. Suzuki, T. Mikami, Y. Okawa, A. Tokoro, S. Suzuki and M. Suzuki: Antitumor effect of hexa-*N*-acetylchitohexaose and chitohexaose. *Carbohydr. Res.*, 151, 403–408 (1986).
2) A. Tokoro, N. Tatewaki, K. Suzuki, T. Mikami, S. Suzuki and M. Suzuki: Growth-inhibitory effect of hexa-*N*-acetylchitohexaose and chitohexaose against Meth-A solid tumor. *Chem. Pharm. Bull.*, 36, 784–790 (1988).
3) K. Tsukada, T. Matsumoto, K. Aizawa, A. Tokoro, R. Naruse, S. Suzuki and M. Suzuki: Antimetastatic and growth-inhibitory effects of *N*-acetylchitohexaose in mice bearing Lewis lung carcinoma. *Jpn. J. Cancer Res.*, 81, 259–265 (1990).
4) A. Tokoro, M. Kobayashi, N. Tatewaki, K. Suzuki, Y. Okawa, T. Mikami, S. Suzuki and M. Suzuki: Protective effect of *N*-acetyl chitohexaose on *Listeria monocytogenes* infection in mice. *Microbiol. Immunol.*, 33, 357–367 (1989).
5) M. Kobayashi, T. Watanabe, S. Suzuki and M. Suzuki: Effect of *N*-acetylchitohexaose against *Candida albicans* infection of tumor-bearing mice. *Microbiol. Immunol.*, 34, 413–426 (1990).
6) N. Dahiya, R. Tewari and G.S. Hoondal: Biotechnological aspects of chitinolytic enzymes: a review. *Appl. Microbiol. Biotechnol.*, 71, 773–782 (2006).
7) M. Scigelova and D.H.G. Crout: Microbial β-*N*-acetylhexosaminidases and their biotechnological applications. *Enzyme Microb. Technol.*, 25, 3–14 (1999).
8) I. Tsigos, A. Martinou, D. Kafetzopoulos and V. Bouriotis: Chitin deacetylases: new, versatile tools in biotechnology. *Trends Biotech.*, 18, 305–312 (2000).
9) D. Kafetzopoulos, A. Martinou and V. Bouriotis: Bioconversion of chitin to chitosan: purification and characterization of chitin deacetylase from *Mucor rouxii*. *Proc. Natl. Acad. Sci. USA*, 90, 2564–2568 (1993).
10) I. Tsigos and V. Bouriotis: Purification and characterization of chitin deacetylase from *Colletotrichum lindemuthianum*. *J. Biol. Chem.*, 270, 26286–26291 (1995).
11) X.D. Gao, T. Katsumoto and K. Onodera: Purification and characterization of chitin deacetylase from *Absidia coerulea*. *J. Biochem.* (Tokyo), 117, 257–263 (1995).
12) K. Tokuyasu, M. Ohnishi-Kameyama and K. Hayashi: Purification and characterization of extracellular chitin deacetylase from *Colletotrichum lindemuthianum*. *Biosci. Biotechnol. Biochem.*, 60, 1598–1603 (1996).
13) K. Ohishi, M. Yamagishi, T. Ohta, M. Motosugi, H. Izumida, H. Sano, K. Adachi and T. Miwa: Purification and properties of two deacetylases produced by *Vibrio algionolyticus* H-8. *Biosci. Biotechnol. Biochem.*, 61, 1113–1117 (1997).
14) Y. Takiguchi and K. Shimahara: *N,N*-diacetylchitobiose production from chitin by *Vibrio anguillarum* strain E-383a. *Lett. Appl. Microbiol.*, 6, 129–131 (1988).
15) K. Kadokura, A. Rokutani, M. Yamamoto, T. Ikegami, H. Sugita, S. Itoi, W. Hakamata, T. Oku and T. Nishio: Purification and characterization of *Vibrio parahaemolyticus* extracellular chitinase and chitin oligosaccharide deacetylase involved in the production of heterodisaccharide from chitin. *Appl. Microbiol. Biotechnol.*, 75, 357–365 (2007).
16) K. Kadokura, Y. Sakamoto, K. Saito, T. Ikegami, T. Hirano, W. Hakamata, T. Oku and T. Nishio: Recombinant chitin oligosaccharide deacetylase from *Vibrio parahaemolyticus*; gene cloning and production in the culture medium of *Escherichia coli* cells. *Biotechnol. Lett.*, 29, 1209–1215 (2007).
17) K. Kadokura, Y. Sakamoto, K. Saito, T. Ikegami, T. Hirano, W. Hakamata, T. Oku and T. Nishio: Production and secretion of a recombinant *Vibrio parahaemolyticus* chitinase by *Escherichia coli*, and its purification from the culture medium. *Biosci. Biotechnol. Biochem.*, 71, 2848–2851 (2007).
18) D.M.F. Van Aalten, B. Synstad, M.B. Brurberg, E. Hough, B. W. Riise, V.G.H. Eijsink and R.K. Wierenga: Structure of two-domain chitotrisidase from *Serratia mercescens* at 1.9-Å resolution. *Proc. Natl. Acad. Sci. USA*, 97, 5842–5847 (2000).
19) K. Ohishi, K. Murase, T. Ohta and H. Etoh: Cloning and sequencing of a chitinase gene from *Vibrio alginolyticus* H-8. *J. Biosci. Bioeng.*, 89, 501–505 (2000).
20) W. Suginta, A. Vongsuwan, C. Songsiriritthigul, H. Prinz, P. Estibeiro, R.R. Duncan, J. Svasti and L.A. Fothergill-Gilmore: An endochitinase A from *Vibrio carchariae*: cloning, expression, mass and sequence analysis, and chitin hydrolysis. *Arch. Biochem. Biophys.*, 424, 171–180 (2004).
21) K. Ohishi, K. Murase, T. Ohta and H. Etoh: Cloning and sequencing of the deacetylase gene from *Vibrio alginolyticus* H-8. *J. Biochem. Bioeng.*, 90, 561–563 (2000).
22) J.P. Chen, F. Nagayama and M.C. Chang: Cloning and expression of a chitinase gene from *Aeromonas hydrophila* in *Escherichia coli*. *Appl. Environ. Microbiol.*, 57, 2426–2428 (1991).
23) N.O. Keyhnani and S. Roseman: Wild-type *Escherichia coli* grows in the chitin disaccharide, *N,N'*-diacetylchitobiose, by expressing the *cel* operon. *Proc. Natl. Acad. Sci. USA*, 94, 14367–14371 (1997).

Vibrio parahaemolyticus が生産するキチン分解酵素の精製，諸性質解析，クローニングおよびリコンビナント酵素のオリゴ糖生産への利用

門倉一成[1]，坂本裕輔[1]，六谷明子[1]，池上孝紀[1]，
平野貴子[1]，山本真広[1]，齋藤香織[1]，袴田　航[1]，
糸井史朗[2]，杉田治男[2]，奥　忠武[1]，西尾俊幸[1]

[1] 日本大学生物資源科学部農芸化学科

[2] 日本大学生物資源科学部海洋生物資源科学科

(252–8510 藤沢市亀井野 1866)

われわれが谷津干潟土壌より単離した *Vibrio parahaemolyticus* KN1699 株は，キチン分解によりヘテロ二糖 [β-*N*-アセチル-D-グルコサミニル-(1,4)-D-グルコサミン (GlcNAc-GlcN)] を生成するユニークな分泌性のキチン分解酵素系を有している．GlcNAc-GlcN の生成メカニズムを調べたところ，本ヘテロ二糖は，GH ファミリー 18 キチナーゼ(*Pa*-Chi)の作用によるキチンからジ-*N*-アセチルキトビオース [$(GlcNAc)_2$] の生成，続いて CE ファミリー 4 キチンオリゴ糖デアセチラーゼ(*Pa*-COD)の作用による $(GlcNAc)_2$ の還元性末端側の糖の脱アセチル化により生成することを明らかにした．二つの酵素を利用してキチンから $(GlcNAc)_2$ と GlcNAc-GlcN を量産するために，大腸菌によるリコンビナント酵素の大量調製について検討した．KN1699 株のゲノムから分泌シグナル配列を含む各 ORF のクローニングを行い，プラスミドを作製した後，大腸菌に導入した．これを用いて各リコンビナント酵素(*Pa*-rChi, *Pa*-rCOD)の発現を行った結果，各酵素を大量に発現させ，さらに培養液中に効率的に分泌させることに成功した．続いて，これら 2 種のリコンビナント酵素を用いたオリゴ糖生産について検討を行った．その結果，*Pa*-rChi 分泌組換え大腸菌を 2% キチン含有培地で培養することで，粉末キチンから $(GlcNAc)_2$ を収率 60% で生産することに成功した．さらに，*Pa*-rCOD 分泌組換え大腸菌から調製した粗酵素溶液を用いて，$(GlcNAc)_2$ から GlcNAc-GlcN を高収率で生産することができた．今後は，生産した GlcNAc-GlcN の機能性について解析する予定で

ある．

＊＊＊＊＊

〔質問〕 (独)農研機構・食総研 徳安

位置特異的に脱アセチル化する酵素は貴重．部分脱アセチル化物のリゾチームによる重合，あるいは逆反応による還元末端のみの選択的アセチル化などについて，可能性があると思うので，是非ご検討いただきたい．

〔答〕

貴重なご意見ありがとうございます．この部分脱アセチル化オリゴ糖および *Pa*-rCOD を使用して検討を行ってみます．

〔質問〕 (独)産総研 矢追

1）IPTG に代わってβ-キチンで発現誘導できたのはなぜか？

2）発酵法を選んだ理由は？

〔答〕

1）β-キチン添加によって起こるキチナーゼの発現誘導の理由については解明中なので明言はできませんが，おそらくβ-キチンの分解によって生成した$(GlcNAc)_2$により発現が誘導されたのではないかと考えています．興味深い現象ですので，今後詳細に検討を行って現象解明を進めていきたいと考えています．

2）発酵法は培養工程でフレッシュな酵素を連続的に供給できるため，キチンのような水不溶性の固形基質には最適な生産法であると考え，この方法を採用しました．

〔質問〕 京大院・生命科学 山本

このデアセチラーゼはキトビオースの還元末端側のアセチル基に特異的に作用するのですか．キチンには作用しないのですか．キチナーゼとデアセチラーゼのそれぞれのリコンビナント酵素を分泌する大腸菌の菌体を用いた発酵法によってオリゴ糖生産はできませんか．

〔答〕

本酵素はキトビオース以外にもキトトリオースにも作用することを確認しています．しかし，キチンには作用しないことを確認しています．それぞれのリコンビナント酵素を分泌させた発酵法での生産については，まだ未検討なので，今後検討を行っていきたいと考えています．

Acta Crystallographica Section F
Structural Biology and Crystallization Communications
ISSN 1744-3091

Cloning, expression and purification of cytochrome c_6 from the brown alga *Hizikia fusiformis* and complete X-ray diffraction analysis of the structure

Hideharu Akazaki,[a] Fumihiro Kawai,[b] Hirotaka Chida,[a] Yuichirou Matsumoto,[a] Mao Hirayama,[a] Ken Hoshikawa,[a] Satoru Unzai,[b] Wataru Hakamata,[a] Toshiyuki Nishio,[a] Sam-Yong Park[a] and Tadatake Oku[a]*

[a]Bio-organic Chemistry Laboratory, Graduate School of Bioresource Sciences, Nihon University, Kameino 1866, Fujisawa-shi, Kanagawa 252-8510, Japan, and [b]Protein Design Laboratory, Graduate School of Integrated Science, Yokohama City University, 1-7-29 Suehiro-cho, Tsurumi, Yokohama 230-0045, Japan

Correspondence e-mail: oku@brs.nihon-u.ac.jp

Received 26 April 2008
Accepted 11 June 2008

PDB Reference: cytochrome c_6, 2zbo, r2zbosf.

The primary sequence of cytochrome c_6 from the brown alga *Hizikia fusiformis* has been determined by cDNA cloning and the crystal structure has been solved at 1.6 Å resolution. The crystal belonged to the tetragonal space group $P4_12_12$, with unit-cell parameters $a = b = 84.58$, $c = 232.91$ Å and six molecules per asymmetric unit. The genome code, amino-acid sequence and crystal structure of *H. fusiformis* cytochrome c_6 were most similar to those of red algal cytochrome c_6. These results support the hypothesis that brown algae acquired their chloroplasts *via* secondary endosymbiosis involving a red algal endosymbiont and a eukaryote host.

1. Introduction

Soluble *c*-type monohaem cytochromes are ubiquitously distributed haem proteins which act as electron carriers in mitochondria, bacteria, algal chloroplasts and cyanobacteria. Cytochrome c_6 is a soluble low-spin haem protein that functions in oxygenic photosynthesis as an electron carrier between cytochrome *f*, which is part of the membrane-embedded cytochrome b_6f complex, and the P700 reaction centre of photosystem I (Kerfeld & Krogmann, 1998). This cytochrome c_6 is classified as a class I *c*-type cytochrome, in which the haem iron has histidine–methionine axial coordination. Plastocyanin is a blue copper protein with the same function as cytochrome c_6. Cytochrome c_6 and plastocyanin have completely different amino-acid sequences and secondary and tertiary structures, but they contain similar acidic and hydrophobic patches on their surface for recognition of their interaction partners (Frazão *et al.*, 1995; Ullmann *et al.*, 1997).

Although chloroplasts are thought to have evolutionally arisen from cyanobacteria (Aitken, 1976), there are differences in the expression and genome coding of cytochrome c_6 in green and red algae. In the green alga *Chlamydomonas reinhardtii*, the gene for cytochrome c_6 exists in the genomic DNA and its coding region is interrupted by two introns (Hill *et al.*, 1991). On the other hand, in the red alga *Porphyra purpurea* the *petJ* gene encoding cytochrome c_6 exists in the chloroplast genome (Reith & Munholland, 1993).

In eukaryotic brown algae, which contain no plastocyanin, photosynthetic electron transport between cytochrome *f* and photosystem I is only performed by cytochrome c_6. It is generally considered that brown algae acquired their chloroplasts *via* secondary endosymbiosis involving a primitive red algal endosymbiont and a nonphotosynthetic eukaryote host (Cavalier-Smith, 2000; McFadden, 1999). Although the physicochemical properties and amino-acid sequences of cytochromes c_6 from the brown algae *Petalonia fascia* and *Alaria esculenta* have been determined (Sugimura *et al.*, 1981; Laycock, 1975), the genome code and tertiary structure of brown algal cytochrome c_6 remain to be studied. In this study, we determined the genome code of the brown algal cytochrome c_6 gene from the brown alga *Hizikia fusiformis*, determined the crystal structure of the protein and compared it with those of cyanobacterial and red and green algal cytochromes c_6.

2. Materials and methods

2.1. Sequence determination

The brown alga *H. fusiformis* was collected in the coastal area off Hayama, Japan. Total RNA was isolated from the brown alga using the RNeasy Plant Mini Kit (Qiagen). Poly(A)$^+$ mRNA and poly(A)$^-$ mRNA were separated from the total RNA using Oligotex-dT30 (Takara). Additional of adenine at the 3′-terminus of poly(A)$^-$ mRNA was carried out for 40 min at 310 K in a reaction mixture containing 2 µg poly(A)$^-$ mRNA, 50 m*M* Tris–HCl pH 7.9, 50 m*M* $MgCl_2$, 10 m*M* $MnCl_2$, 500 m*M* NaCl, 2.5 m*M* DTT, 0.5% BSA, 1 m*M* ATP, 121 U ribonuclease inhibitor and 1.5 U poly(A) polymerase (Takara). First-strand cDNA was synthesized using a 1st Strand cDNA Synthesis Kit with AMV Reverse Transcriptase (Life Science Inc.) and the oligonucleotide primer 5′-CGGGATCC$(T)_{25}$-3′, designated primer P1 (reverse). To obtain the clone encoding the 3′-region of cytochrome c_6 from *H. fusiformis*, we designed the degenerate oligonucleotide primer P2 (forward), 5′-AAYTGYGCIGCIGCIT-GYCAYGCI-3′, based on the highly conserved residues around the haem *c* motif (Asn-Cys-Ala-Ala-Cys-His-Ala) of cytochrome c_6 from the cyanobacteria *Synechocystis* PCC6803 and *Anabaena* 7119, the green alga *C. reinhardtii*, the euglena *Euglena gracillis* and the cyanelle *Cyanophora paradoxa*. PCR products were subcloned into a pGEM T-Easy vector (Promega). DNA sequencing was performed by the dideoxy chain-termination method using a Thermo Sequence fluorescent-labelled primer cycle sequencing kit with 7-deaza-dGTP (Amasham) and an automated DSQ 2000L DNA sequencer (Shimadzu, Japan). The first-strand cDNA from *H. fusiformis* were dC-tailed at their 3′-ends using the 5′ RACE system for Rapid Amplification of cDNA Ends Reagent Assembly v.2.0 (Life Technologies Inc.). The 5′-region of the cytochrome c_6 gene from *H. fusiformis* was amplified by the polymerase chain reaction (PCR) using a forward primer complementary to the dC tail [P3, 5′-GGCCACGCGTCGACTAGTAC$(G)_{16}$-3′] and a gene-specific primer designed based on the 3′-region sequences of the cytochrome c_6 cDNA (Hf1, 5′-TCAGGCATAATAATAACATTATTACCGCC-3′). The PCR product was subcloned and sequenced by the same methods as used in 3′ RACE. Genome DNA from *H. fusiformis* was extracted using Isoplant II (Nippon Gene). To obtain the genome sequence of *H. fusiformis* cytochrome c_6, we designed gene-specific primers for amplification of the full-length cytochrome c_6 gene on the basis of the cDNA sequence of cytochrome c_6 (Hf2, 5′-ATGGGGGGGTGGAAAATTTATTATT-3′, forward; Hf3, 5′-TCAACGTTCCAGGTCCAATAATATCATAA-3′, reverse). The PCR product was subcloned and sequenced according to 3′ RACE.

2.2. Construction of expression vector

Construction and overproduction of the cytochrome c_6 gene (*petJ*) in *Escherichia coli* was performed according to the method described by Satoh *et al.* (2002) with slight modifications. The mature cytochrome c_6 sequence was amplified using the forward primer ExP1 (5′-CATGCCATGGGCTGATATTAATCATGGAG-3′) corresponding to codons for the amino-acid residues of the cytochrome c_6 N-terminal region and the reverse primer ExP2 (5′-GCGGATCCTTAGT-TCCAACTCTTTTCAG-3′) corresponding to codons for the amino-acid residues of the C-terminal region. The amplified mature cytochrome c_6 sequence was ligated to the *pelB* signal sequence adapter (Genset Co. Ltd). The resulting *pel*B–cytochrome c_6 hybrid gene was cloned into *Nde*I–*Bam*HI sites of pET22b(+) (Novagen Co. Ltd) to construct the plasmid pET22bHfc6.

The cytochrome *c* maturation genes *ccmA–H* were amplified using the polymerase chain reaction from *E. coli* MC1061 genomic DNA using the forward primer P3, 5′-CCAGAATTCGGTTGCCGC-GAAGATGCAT-3′, corresponding to upstream of the *ccmA* gene from the *E. coli* K12 MG1655 genome sequence (AE000309), and the reverse primer P4, 5′-TTCCTGCAGCAACGCGGGGCACAATA-AA-3′, corresponding to downstream of the *ccmH* gene. The resulting *ccmA–H* gene was cloned into the *Eco*RI–*Pst*I sites of pSTV28 (Takara Shuzo Co.) to create the plasmid pSTV28*ccmA–H*.

2.3. Protein expression and purification

For the overproduction of *H. fusiformis* cytochrome c_6, both pET22bHfc6 and pSTV28*ccmA–H* were co-introduced into *E. coli* BL21 (DE3). Transformed *E. coli* cells were grown in 1 l Luria–Bertani (LB) medium supplemented with 100 mg l^{-1} ampicillin and 20 mg l^{-1} chloramphenicol at 303 K for 36 h. Cells were harvested by centrifugation at 6000*g* (277 K) for 5 min. The pellet was resuspended in 80 ml PBS buffer and disrupted using a high-pressure homogenizer (Mini Lab 8.30H, Rannie). The suspension was fractionated with ammonium sulfate (40–80% saturation). The precipitate was dissolved in a small amount of 20 m*M* sodium acetate buffer pH 5.5 and dialyzed against the same buffer. The sample was applied onto a DE52 cellulose column (Whatman, 2.0 × 40.0 cm) equilibrated with 20 m*M* sodium acetate buffer pH 5.5. After the column had been washed with the same buffer, the proteins were eluted using a linear gradient of sodium acetate pH 5.5 (20–200 m*M*). Fractions containing cytochrome c_6 were pooled and dialyzed against 20 m*M* sodium acetate buffer pH 5.5 and the dialyzed sample was applied onto a Poros HQ/20 column (Applied Biosystems) previously equilibrated with the same buffer. After the column had been washed with the same buffer, the proteins were eluted with an NaCl gradient (0–500 m*M*) in the same buffer. The sample thus obtained was used as purified recombinant *H. fusiformis* cytochrome c_6. The degree of purity was confirmed by tricine SDS–PAGE (Schägger & von Jagow, 1987) and UV–visible spectroscopy. UV–visible spectra of *H. fusiformis* cytochrome c_6 were measured with a Hitachi U3310 spectrophotometer using quartz cuvettes of 1.0 cm path length. The concentration of the cytochrome c_6 was determined spectrophotometrically from the pyridine ferrohaemochrome spectrum (550 nm, 29.1 mM^{-1} cm^{-1}). Potassium ferricyanide and sodium dithionite were used as the oxidant and the reductant, respectively.

2.4. Crystallization and refinement

The purified protein was dissolved in 10 m*M* sodium phosphate buffer pH 7.0 to prepare a concentrated protein solution of 20 mg ml^{-1}. Initial crystals were obtained using the Wizard I random sparse-matrix crystallization screen (Emerald BioSystem). *H. fusiformis* cytochrome c_6 was crystallized by vapour diffusion using the hanging-drop method at 293 K. Each drop consisted of 2 µl protein solution and 2 µl reservoir solution. An initial crystal of *H. fusiformis* cytochrome c_6 grew within a week using condition No. 33 [2.0 *M* $(NH_4)_2SO_4$, 0.1 *M* CAPS pH 10.5 and 0.2 *M* Li_2SO_4]. To improve the quality of the crystal, further screening for crystallization was performed and crystals were obtained reproducibly using 0.1 *M* CAPS pH 10.5, 0.2 *M* Li_2SO_4, 2.2 *M* $(NH_4)_2SO_4$ and 3% glycerol. X-ray diffraction data were collected on BL-5A, Photon Factory, Tsukuba, Japan. The data set was processed with *HKL*-2000 and scaled with *SCALEPACK* (Otwinowski & Minor, 1997). The structure of *H. fusiformis* cytochrome c_6 was determined by molecular replacement using the program *MOLREP* (Collaborative Computational Project, Number 4, 1994). The search model used was

Table 1
Crystal parameters and data-collection and structure refinement.

Values in parentheses are for the outer shell (1.66–1.60 Å).

Data-collection statistics	
Temperature (K)	100
Resolution range (Å)	50.0–1.6
Space group	$P4_12_12$
Unit-cell parameters (Å)	$a = b = 84.578$, $c = 232.911$
Reflections (measured/unique)	699906/107513 (9592)
Completeness (%)	95.6 (86.8)
R_{merge}† (%)	4.8 (23.5)
Redundancy	6.6 (3.5)
Mean $I/\sigma(I)$	20.5
Mosaicity	0.33
Refinement statistics	
Resolution range (Å)	20.0–1.6
σ Cutoff/reflections used	0.0/107239
R factor/R_{free}‡ (%)	18.4/20.9
R.m.s.d. bond lengths (Å)/bond angles (°)	0.011/1.165
B factors (Å^2)	
Average	22.4
Protein	21.1
Haem	14.8
Water	34.0
Sulfate	40.5
Ramachandran plot	
Residues in most favourable region (%)	82.7
Residues in additional allowed region (%)	16.0
Residues in disallowed region (%)	1.3

† $R_{merge} = \sum_{hkl}\sum_i |I_i(hkl) - \langle I(hkl)\rangle| / \sum_{hkl}\sum_i I_i(hkl)$, where $I_i(hkl)$ is the intensity of an observation and $\langle I(hkl)\rangle$ is the mean value for the unique reflection; summations are over all reflections. ‡ R factor $= \sum_h |F_o(h) - F_c(h)| / \sum_h F_o(h)$, where F_o and F_c are the observed and calculated structure-factor amplitudes, respectively. The free R factor was calculated using 5% of the data, which were excluded from the refinement.

Porphyra yezoensis cytochrome c_6 (Yamada *et al.*, 2000). The structure of *H. fusiformis* cytochrome c_6 was refined with *REFMAC* from the *CCP*4 program suite. Water molecules were added using a water-pick script in *CNS* and refinement was continued using *REFMAC*5 (Collaborative Computational Project, Number 4, 1994). The final model obtained had an R factor of 18.4% and a free R factor of 20.9%. Manual model building was carried out using *Coot* (Emsley & Cowtan, 2004). Solvent molecules were placed at positions where spherical electron-density peaks were found above 1.5σ in the $|2F_o - F_c|$ map and above 3.0σ in the $|F_o - F_c|$ map and where stereochemically reasonable hydrogen bonds were allowed. A summary of the data-collection and refinement statistics is given in Table 1.

3. Results and discussion

3.1. Sequence of *H. fusiformis* cytochrome c_6

To elucidate the genome code of a cytochrome c_6 gene from a brown alga, we determined the protein cDNA from the brown alga *H. fusiformis* as shown in Fig. 1 (Genbank accession No. AB105058). *H. fusiformis* cytochrome c_6 genes were amplified using cDNA, which was performed by the reverse transcription of poly(A)$^-$ mRNA. The polyadenylation signal sequences (AAUAAA) necessary for the addition of polyadenylic acid were not included in the 3′-region of the cytochrome c_6 gene from *H. fusiformis*, but the 3′-regions of the cDNA of the cytochrome c_6 that contained the sequence that can form a stem-loop structure that stabilizes mRNA were transcribed from the chloroplast genome (Drager *et al.*, 1996; Yang & David, 1997). The gene that was transcribed from the chloroplast genome does not add polyadenylic acids (Sagher *et al.*, 1976). Generally, the addition of polyadenylic acids that participate in mRNA stability occurs after transcription inside the nucleus (Darnell *et al.*, 1971; O'Hara *et al.*, 1995). The Shine–Dalgano (SD) sequence, a 16S-ribosomal RNA-binding site that is rich in purine 3–9 bases upstream of the initiation codon of prokaryotic cell mRNA (Bonham-Smith &

Figure 1
Nucleotide sequence and deduced amino-acid sequence of the cDNA encoding cytochrome c_6 from the brown alga *H. fusiformis*. The amino-acid residues numbered −1 to −24 and 1–86 constituted the putative transit sequence and the mature peptide sequence, respectively. Underlined and double-underlined nucleotides indicate the initiation codon and termination codon, respectively. Nucleotides underlined with a wavy line indicate the Shine–Dalgarno-like sequence. The open arrowhead indicates the putative transit-peptide cleavage site. The arrows indicates the primers used. The residues marked with asterisks and the amino-acid residues in italics (−1 to −3) correspond to the haem *c* motif (Cys-*X*-*X*-Cys-His) and cleavage motif (Val-*X*-Ala), respectively. The box indicates the stem-loop structure-formation sequence.

Bourque, 1989), was present ten bases upstream of the initiation codon in the *H. fusiformis* cytochrome c_6 gene (Fig. 1). There were also no SD sequences in the cytochrome c_6 genes of the green alga *C. reinhardtii* (Merchant & Bogorad, 1987), the euglena *Euglena gracilis* (Vacula *et al.*, 1999) and the cyanelle *Cyanophora paradoxa* (Steiner *et al.*, 2000) that are encoded in the nuclear genome. We obtained a genomic DNA clone of approximately 730 bp that was amplified using primers constructed based on cDNA sequences (Fig. 1). The gene that encodes cytochrome c_6 was not inserted with an intron. The green alga *C. reinhardtii* gene encoding cytochrome c_6 has been reported to have its coding region interrupted by two introns (Hill *et al.*, 1991). Genes encoded in nuclear genomes are usually inserted with introns (The Arabidopsis Initiative, 2000), but genes encoded in chloroplast genomes do not have these insertions (Shinozaki *et al.*, 1986). These results showed that the cytochrome c_6 gene from the brown alga *H. fusiformis* was encoded in the chloroplast genome. At present, only red and brown algae have been reported to have a cytochrome c_6 gene encoded in the chloroplast genome.

3.2. Protein expression and purification

E. coli BL21 (DE3) harbouring both pET22bHfc6 and pSTV28*ccmA–H* was used as a source of recombinant *H. fusiformis* cytochrome c_6. Recombinant *H. fusiformis* cytochrome c_6 was purified by ammonium sulfate pecipitation and two-step anion-exchange chromatography. The degree of homogeneity was confirmed by tricine SDS–PAGE and UV–visible spectroscopy. After initial purification by anion-exchange chromatography, tricine SDS–PAGE analysis displayed a predominant cytochrome c_6 band and a minor band and the fractions with an $A_{275}/A_{552.5}$ ratio lower than 2.0 were pooled and concentrated. After a second chromatography purification step, tricine SDS–PAGE analysis showed only the cytochrome c_6 band and the purification ratio ($A_{275}/A_{552.5}$) of *H. fusiformis* cytochrome c_6 was 0.90, which was similar to that of other cytochromes c_6.

The protein consists of 86 amino acids and one *c*-type haem and its molecular weight was calculated to be 9762.4 Da. From SDS–PAGE analysis a value of 8.0 kDa was obtained, which is somewhat lower than that deduced from the sequence (Fig. 2*a*). Similar discrepancies have been observed in other small negatively charged proteins, such as the green alga *Monoraphidium braunii* cytochrome c_6 and plastocyanin (Campos *et al.*, 1993).

The UV–visible spectra of reduced and oxidized recombinant *H. fusiformis* cytochrome c_6 are shown in Fig. 2(*b*). In the reduced form, the α, β, γ (Soret) and δ absorption maxima peaks appear at 552.5, 522.0, 416.0 and 318.0 nm, respectively. For the oxidized form of the cytochrome c_6, the $\alpha + \beta$ and γ (Soret) absorption maxima peaks were 528.0 and 408.5 nm, respectively; a shoulder peak at 695.0 nm, indicating His–Fe–Met coordination, was observed (Fig. 2*b*, inset).

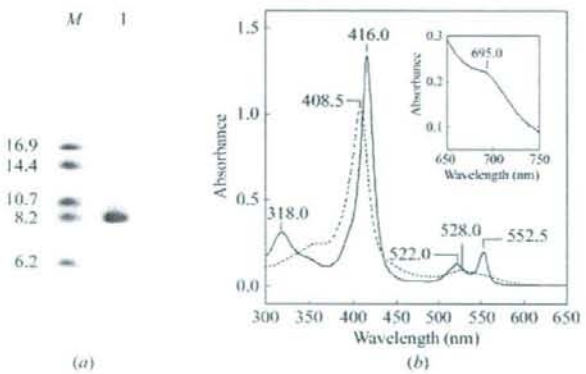

Figure 2
SDS–PAGE analysis and UV–visible spectra of purified *H. fusiformis* cytochrome c_6. (*a*) Proteins were analysed on 16.5% tricine SDS–PAGE and stained with Coomassie Blue. Lane *M*, molecular-weight markers (kDa); lane 1, purified *H. fusiformis* cytochrome c_6. (*b*) UV–visible spectra of dithionite-reduced (solid line) and ferricyanide-oxidized (dotted line) forms of *H. fusiformis* cytochrome c_6 (10 μM) were measured in 10 m*M* sodium phosphate pH 7.0 at 298 K. The inset shows the 695 nm band of the oxidant form at 500 μM.

3.3. Crystallization of *H. fusiformis* cytochrome c_6

A crystallization droplet was prepared by mixing 2 µl protein solution (20 mg ml^{-1} protein) in 10 m*M* sodium phosphate buffer pH 7.0 and 2 µl reservoir solution consisting of 0.1 *M* CAPS pH 10.5, 0.2 *M* Li_2SO_4, 2.2 *M* $(NH_4)_2SO_4$ and 3% glycerol and was equilibrated against 500 µl of the same reservoir solution at 293 K. Diffraction-quality crystals appeared within a week (Fig. 3). This reservoir solution used for *H. fusiformis* cytochrome c_6 is somewhat similar to that used for cytochrome c_6 from the cyanobacterium *Arthrospira maxima* [reservoir solution containing 0.1 *M* Tris pH 7.8, 0.2 *M* Li_2SO_4, 2.2 *M* $(NH_4)_2SO_4$ and 1% glycerol (Sawaya *et al.*, 2001)], but few similarities were found between the reservoir solutions used for *H. fusiformis* cytochrome c_6 and those used for other algal and cyanobacterial cytochromes c_6 (Kerfeld *et al.*, 1995; Frazão *et al.*, 1995; Schnackenberg *et al.*, 1999; Yamada *et al.*, 2000; Dikiy *et al.*, 2002; Worrall *et al.*, 2007).

3.4. Overall structure of *H. fusiformis* cytochrome c_6

The crystal structure of *H. fusiformis* cytochrome c_6 has been determined at 1.6 Å resolution. This is the first cytochrome c_6 crystal structure for a brown secondary symbiotic alga. The crystal belonged to space group $P4_12_12$, with unit-cell parameters $a = b = 84.58$, $c = 232.9$ Å and six molecules (*A*, *B*, *C*, *D*, *E* and *F*) per asymmetric unit (Fig. 4*a*). These six molecules could be superimposed with main-chain root-mean-square deviation (r.m.s.d.) values of 0.1–0.4 Å, as determined using the *DALI* program (Holm & Park, 2000). The hexamer contains four sulfate ions which may be derived from the ammonium sulfate and lithium sulfate included in the crystallization solution. The cytochrome c_6 hexamer was formed of a dimer of trimers (*ABC* and *DEF* trimers; Fig. 4*b*). An intermolecular hydrogen bond was formed in the *ABC* trimer between each pair of molecules

Figure 3
Crystal of *H. fusiformis* cytochrome c_6 grown in 0.1 *M* CAPS pH 10.5, 0.2 *M* Li_2SO_4, 2.2 *M* $(NH_4)_2SO_4$ and 3% glycerol.

in the trimer through Ala60 N and Arg64 O and one sulfate ion was centred between the Arg64 side chains of the three molecules (Fig. 4*c*). This arrangement of a sulfate ion enclosed by a basic amino-acid residue has been also found in the crystal structure of *Hydrogenobacter thermophilus* cytochrome c_{552} (Travaglini-Allocatelli *et al.*, 2005). Considering that the crystals of *H. fusiformis* cytochrome c_6 were obtained in the presence of sulfate ions, the sulfate ions were convenient for crystallization and might contribute to crystal-packing stabilization by neutralization of charge repulsion in this region. Therefore, we deduce that the crystallographic hexamer is a nonphysiological crystal-packing artifact. An intermolecular hydrogen bond was formed between each pair of molecules of the second trimer through the C-terminal Asn86 $N^{\delta2}$ and Asn86 OX (Fig. 4*c*). Hydrogen bonds between the two trimers were formed between Asn22 $O^{\delta1}$ of the *ABC* trimer and Arg64 $N^{\eta2}$ of the *DEF* trimer.

An oligomeric arrangement of molecules has been found in the crystal structures of other cytochromes c_6. A trimeric arrangement of molecules has been found in the structures of cytochrome c_6 from *C. reinhardtii* form I (Kerfeld *et al.*, 1995) and *M. braunii* (Frazão *et al.*, 1995). The proteins from *Scenedesmus obliquus* (Schnackenberg *et al.*, 1999), *A. maxima* (Sawaya *et al.*, 2001) and *Phormidium laminosum* (Worrall *et al.*, 2007) have been crystallized as dimers. These oligomers of cytochromes c_6 were formed by the packing of different molecules and were not superimposed. It has been reported that the observed differences in oligomerization between various cytochromes c_6 may be determined by subtle differences in their surface electrostatic potential properties (Dikiy *et al.*, 2002). In

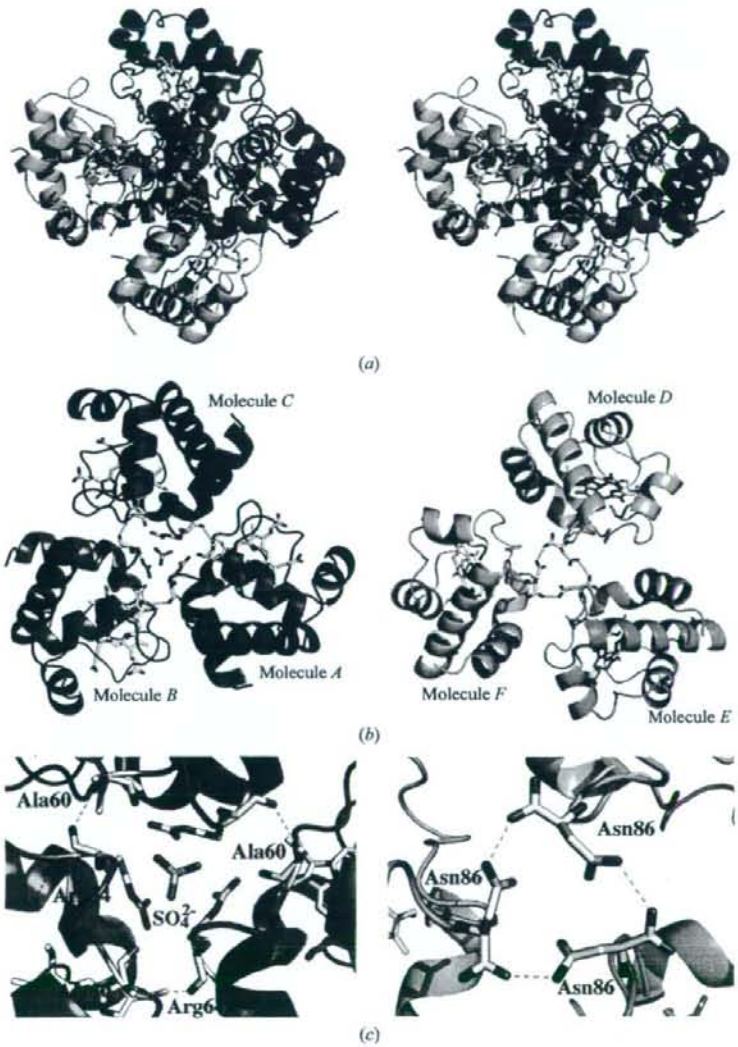

Figure 4
H. fusiformis cytochrome c_6 hexamer. Six protein molecules are displayed, with each molecule in a different colour (red, molecule *A*; marine, molecule *B*; magenta, molecule *C*; lemon, molecule *D*; green, molecule *E*; cyan, molecule *F*). The amino-acid residues and haem group are represented by a stick model with atom-specific colours: white, carbon; blue, nitrogen; red, oxygen; yellow, sulfur; iron, orange. This figure was drawn with *PyMOL*.

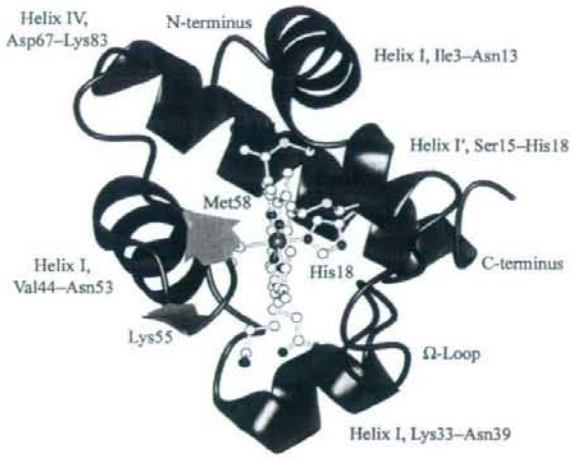

Figure 5
Overall structure of cytochrome c_6 from the brown alga *H. fusiformis*. The α-helix (marine) and β-sheet (green) are indicated as a cartoon model. Cys14, Cys17, His18, Met58 and haem are represented using a ball-and-stick model in the same colour scheme used in Fig. 1. This figure was drawn with *CCP*4 (Collaborative Computational Project, Number 4, 1994).

contrast, the cytochromes c_6 from *P. yezoensis* (Yamada *et al.*, 2000) and *Cladophora glomerate* (Dikiy *et al.*, 2002) are monomeric in the crystal.

The structure of *H. fusiformis* cytochrome c_6 belongs to the class I *c*-type cytochromes, which are composed of four α-helices and tight turns (Fig. 5). The protein consists of a single polypeptide chain folded around the haem prosthetic group. The secondary structures have been classified according to the criteria of Kabsch & Sander (1983). Four α-helices, Asp2–Asn13 (I), Ser15–His18 (I'), Lys33–Ala38 (II), Ile44–Asn53 (III) and Asp67–Lys83 (IV), are found as elements of a regular secondary structure, with helices I and IV overlapping at about 90° (Fig. 3). A two-stranded antiparallel β-sheet was formed with two interchain hydrogen bonds between Lys55 and Met58, which form a type II' β-turn with Asn56 and Ala57. A short β-sheet has commonly been observed in the structures of cyanobacterial, green and red algal cytochromes c_6.

3.5. Structural comparison between *H. fusiformis* and other cytochromes c_6

The crystal structures of four cytochromes c_6 from the eukaryotic green algae *C. reinhardtii* (Kerfeld *et al.*, 1995), *M. braunii* (Frazão *et al.*, 1995), *S. obliquus* (Schnackenberg *et al.*, 1999) and *C. glomerata* (Dikiy *et al.*, 2002), of one from the eukaryotic red alga *P. yezoensis* (Yamada *et al.*, 2000) and of two from the prokaryotic cyanobacteria *A. maxima* (Sawaya *et al.*, 2001) and *P. laminosum* (Worrall *et al.*, 2007) have been determined. They are composed of 85–90 amino acids and their main secondary-structural elements are α-helices wrapping around the haem prosthetic group. An amino-acid sequence comparison of *H. fusiformis* cytochrome c_6 with those from *C. reinhardtii*, *M. braunii*, *C. glomerata*, *S. obliquus*, *P. yezoensis*, *A. maxima* and *P. laminosum* revealed similarities of 46.67, 47.78, 45.05, 47.19, 72.09, 53.33 and 59.77%, respectively (Fig. 6) and the amino-acid sequence of *H. fusiformis* cytochrome c_6 is most similar to that of *P. yezoensis* cytochrome c_6. The main-chain r.m.s.d.s between *H. fusiformis*, *C. reinhardtii*, *P. yezoensis* and *A. maxima* cytochromes c_6 are 0.5–1.1 Å, as determined using the *DALI* program (Holm & Park, 2000). A C^{α} trace of *H. fusiformis* cytochrome c_6 shows a high overall similarity between the green algal and cyanobacterial cytochromes c_6, as well as subtle differences (Fig. 7). The largest deviation in the C^{α} trace between the brown alga *H. fusiformis* cytochrome c_6 and green algal and cyanobacterial cytochromes c_6 was found in the second interconnecting loop (Gln40–Ser43; Fig. 7). The green algal and cyanobacterial cytochromes c_6 have a small insertion of 2–4 amino acids in this region compared with *H. fusiformis* cytochrome c_6. The loop region in *H. fusiformis* cytochrome c_6 resembles that in cytochrome c_6 from the red alga *P. yezoensis*, which also lacks two amino acids in this region compared with green algal and cyanobacterial cytochromes c_6. Considering that the loop region of cytochromes c_6 has a poorly conserved amino-acid sequence compared with other regions, this region may have no common biological functional role. In the structure of other cytochromes, functional roles have not been reported for this region.

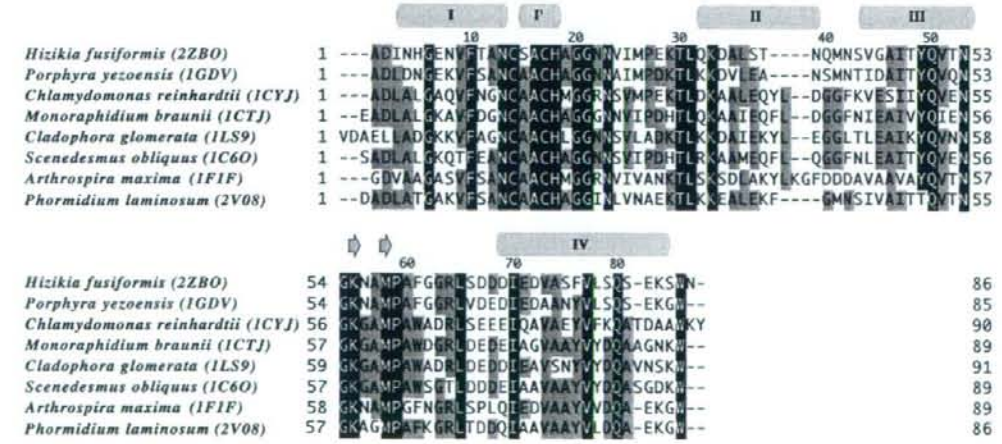

Figure 6
Aligned amino-acid sequences of cytochromes c_6 with reported crystal structures. The conserved and semi-conserved amino-acid residues among the six algal species and two cyanobacterial species are indicated by black and grey boxes, respectively. The haem ligands and the residues forming the acidic patch of the exposed surface are shown in yellow and red, respectively. The secondary structure of cytochrome c_6 from *H. fusiformis* is indicated: orange cylinders, α-helices; blue arrows, β-sheets.

Figure 7
Superimposition of the C$^{\alpha}$ traces of oxidized cytochromes c_6 from the brown alga *H. fusiformis* (orange; PDB code 2zbo), the red alga *P. yezoensis* (red; PDB code 1gdv), the green alga *C. reinhardtii* (green; PDB code 1cyj) and the cyanobacterium *A. maxima* (marine; PDB code 1f1f). The alignment was prepared using the *DALI* program (Holm & Park, 2000).

In this study, we showed that the cytochrome c_6 gene from the brown alga *H. fusiformis* was encoded in the chloroplast genome. To date, the cytochrome c_6 gene has only been found to be encoded in the chloroplast genome in red and brown algae. The amino-acid sequence and tertiary structure of *H. fusiformis* cytochrome c_6 were very similar to those of a red algal cytochrome c_6 rather than those of green algal cytochromes c_6. The present results support the hypothesis that brown algae gained their chloroplasts *via* secondary endosymbiosis involving a primitive red algal endosymbiont and a nonphotosynthetic eukaryote host.

We thank Messrs Daisuke Tamura, Naoya Terunuma and Masaki Hosokawa and Mses Ayako Ohsuzu, Ayumi Hisamitsu and Kasumi Suzuki of Nihon University for the expression and purification of *H. fusiformis* cytochrome c_6. This work was supported in part by a Nihon University Multidisciplinary Research Grant for 2008.

References

Aitken, A. (1976). *Nature (London)*, **263**, 793–796.
Bonham-Smith, P. C. & Bourque, D. P. (1989). *Nucleic Acids Res.* **17**, 2057–2080.
Campos, A. P., Aguiar, A. P., Hervás, M., Regalla, M., Navarro, J. A., Ortega, J. M., Xavier, A. V., De La Rosa, M. A. & Teixeira, M. (1993). *Eur. J. Biochem.* **216**, 329–341.
Cavalier-Smith, T. (2000). *Trends Plant Sci.* **5**, 174–182.
Collaborative Computational Project, Number 4 (1994). *Acta Cryst.* D**50**, 760–763.
Darnell, J. E., Philipson, L., Wall, R. & Adesnic, M. (1971). *Science*, **174**, 507–510.
Dikiy, A., Carpentier, W., Vandenberghe, I., Borsari, M., Safarov, N., Dikaya, E., Van Beeumen, J. & Ciurli, S. (2002). *Biochemistry*, **41**, 14689–14699.
Drager, R. G., Zeidler, M., Simpson, C. L. & Stern, D. B. (1996). *RNA*, **2**, 652–663.
Emsley, P. & Cowtan, K. (2004). *Acta Cryst.* D**60**, 2126–2132.
Frazão, C., Soares, C. M., Carrondo, M. A., Pohl, E., Dauter, Z., Wilson, K. S., Hervás, M., Navarro, J. A., De La Rosa, M. A. & Sheldrick, G. M. (1995). *Structure*, **3**, 1159–1169.
Hill, K. L., Li, H. H., Singer, J. S. & Merchant, S. (1991). *J. Biol. Chem.* **266**, 15060–15067.
Holm, L. & Park, J. (2000). *Bioinformatics*, **16**, 566–567.
Kabsch, W. & Sander, C. (1983). *Biopolymers*, **22**, 2577–2637.
Kerfeld, C. A., Anwar, H. P., Interrante, R., Merchant, S. & Yeates, T. O. (1995). *J. Mol. Biol.* **250**, 627–647.
Kerfeld, C. A. & Krogmann, D. W. (1998). *Annu. Rev. Plant Physiol. Plant Mol. Biol.* **49**, 397–425.
Laycock, M. V. (1975). *Biochem. J.* **149**, 271–279.
McFadden, G. I. (1999). *J. Eukaryot. Microbiol.* **46**, 339–346.
Merchant, S. & Bogorad, L. (1987). *J. Biol. Chem.* **262**, 9062–9067.
O'Hara, E. B., Chekanova, J. A., Ingle, C. A., Kushner, Z. R., Peters, E. & Kushner, S. R. (1995). *Proc. Natl Acad. Sci. USA*, **92**, 1807–1811.
Otwinowski, Z. & Minor, W. (1997). *Methods Enzymol.* **276**, 307–326.
Reith, M. & Munholland, J. (1993). *Plant Cell*, **5**, 465–475.
Satoh, T., Itoga, A., Isogai, Y., Kurihara, M., Yamada, S., Natori, M., Suzuki, N., Suruga, K., Kawachi, R., Arahira, M., Nishio, T., Fukazawa, C. & Oku, T. (2002). *FEBS Lett.* **531**, 543–547.
Sagher, D., Grosfeld, H. & Edelman, M. (1976). *Proc. Natl Acad. Sci. USA*, **73**, 722–726.
Sawaya, M. R., Krogmann, D. W., Serag, A., Ho, K. K., Yeates, T. O. & Kerfeld, C. A. (2001). *Biochemistry*, **40**, 9215–9225.
Schägger, H. & von Jagow, G. (1987). *Anal. Biochem.* **166**, 368–379.
Schnackenberg, J., Than, M. E., Mann, K., Wiegand, G., Huber, R. & Reuter, W. (1999). *J. Mol. Biol.* **290**, 1019–1030.
Shinozaki, K. *et al.* (1986). *EMBO J.* **5**, 2043–2049.
Steiner, J. M., Serrano, A., Allmaier, G., Jakowitsch, J. & Löffelhardt, W. (2000). *Eur. J. Biochem.* **267**, 4232–4241.
Sugimura, Y., Hase, T., Matsubara, H. & Shimokoriyama, M. (1981). *J. Biochem. (Tokyo)*, **90**, 1213–1219.
The Arabidopsis Initiative (2000). *Nature (London)*, **408**, 796–815.
Travaglini-Allocatelli, C., Gianni, S., Dubey, V. K., Borgia, A., Di Matteo, A., Bonivento, D., Cutruzzolà, F., Bren, K. L. & Brunori, M. (2005). *J. Biol. Chem.* **280**, 25729–25734.
Ullmann, G. M., Hauswald, M., Jensen, A., Kostic, N. M. & Knapp, E. W. (1997). *Biochemistry*, **36**, 16187–16196.
Vacula, R., Steiner, J. M., Krajcovic, J., Ebringer, L. & Löffelhardt, W. (1999). *DNA Res.* **6**, 45–49.
Worrall, J. A., Schlarb-Ridley, B. G., Reda, T., Marcaida, M. J., Moorlen, R. J., Wastl, J., Hirst, J., Bendall, D. S., Luisi, B. F. & Howe, C. J. (2007). *J. Am. Chem. Soc.* **129**, 9468–9475.
Yamada, S., Park, S.-Y., Shimizu, H., Koshizuka, Y., Kadokura, K., Satoh, T., Suruga, K., Ogawa, M., Isogai, Y., Nishio, T., Shiro, Y. & Oku, T. (2000). *Acta Cryst.* D**56**, 1577–1582.
Yang, J. & David, B. S. (1997). *J. Biol. Chem.* **272**, 12874–12880.